ROBUST POWER SYSTEM STABILIZER FOR MULTI-MACHINE POWER NETWORKS USING TUNICATE SWARM ALGORITHM AND EQUILIBRIUM OPTIMIZER

by

JAHID HASAN TAYEB

SAYED MD. ABRAR GANI

BACHELOR OF SCIENCE IN ELECTRICAL AND ELECTRONIC ENGINEERING

Department of Electrical and Electronic Engineering
INTERNATIONAL ISLAMIC UNIVERSITY CHITTAGONG

APRIL 2022

ROBUST POWER SYSTEM STABILIZER FOR MULTI-MACHINE POWER NETWORKS USING TUNICATE SWARM ALGORITHM AND EQUILIBRIUM OPTIMIZER

by

JAHID HASAN TAYEB

SAYED MD. ABRAR GANI

A thesis/project
submitted as partial fulfilment of the requirement for the degree of

BACHELOR OF SCIENCE IN ELECTRICAL AND ELECTRONIC ENGINEERING

Department of Electrical and Electronic Engineering
INTERNATIONAL ISLAMIC UNIVERSITY CHITTAGONG

APRIL 2022

CERTIFICATE OF APPROVAL

The thesis/project entitled as "**Robust Power System Stabilizer for Multi-Machine Power Networks Using Tunicate Swarm Algorithm and Equilibrium Optimizer**" submitted by **Jahid Hasan Tayeb and Sayed Md. Abrar Gani**, bearing Matric ID. **ET171064 and ET171065** of session **Spring 2017**, to the Department of Electrical and Electronic Engineering, International Islamic University Chittagong, has been accepted as satisfactory in partial fulfilment of the requirements for the degree of bachelor of science in engineering and approved for the examination held on **16th April, 2022**.

____

Supervisor
Engr. Md. Rashidul Islam
Assistant Professor
Department of Electrical and Electronic Engineering
International Islamic University Chittagong (IIUC)

DECLARATION

This work has been done entirely by myself, and no part of the work included in this thesis/project has been submitted elsewhere for the granting of any degree or credential.

Jahid Hasan Tayeb

Sayed Md. Abrar Gani

ACKNOWLEDGMENT

All praise and gratitude go to allah, the almighty, the most merciful, the most beneficent, for assisting us in completing this task.

This thesis stayed on track and was finished with the help and encouragement of the following people. At the end of our thesis, we'd like to thank everyone who helped make this thesis possible and an experience we'll never forget. First of all, we want to thank our supervisor, Engr. Md. Rashidul Islam, for giving us the space and tools we needed to do our research. Without his direction, help, and support, this work would not have been possible. With his help, we got through many tough situations and learned a lot. We would like to express our deep gratitude to him for his advice, guidance, patience and understanding throughout whole period of conducting the research. We are especially indebted to him in this regard as we got the chance to develop our skill on how to conduct research and use statistical software. We also want to thank our co-advisor, Dr. Md. Shafiullah, for his great help with this research. At this point in our lives, we think about how far we've come because of the sacrifices my parents made and how hard they worked through pain, tears, and constant prayer. We shouldn't forget to thank our brothers and sisters for always being there for us with love, support, understanding, and good wishes. We're grateful to the faculty of the EEE department for their help in this matter. We owe all the authors and researchers whose work we used to plan the research and write this dissertation. Last but not least, we'd like to thank everyone who helped us directly or indirectly with our thesis. Everyone who wasn't thanked in this list is also thanked.

Author

ABSTRACT

Low-frequency oscillations (LFO) in power systems can cause a lot of interruptions, which can cause the system to become unstable. Low-frequency oscillation has frequently been reduced and long-term stability improved through the use of stabilizers in power systems. This thesis represents two new methods of modeling robust power system stabilizers (PSS) for multi-machine networks using the Equilibrium optimizer (EO) and tunicate swarm algorithm (TSA). To improve system damping, a damping ratio-based goal function is considered, and a commonly utilized traditional lead-lag type PSS structure is employed. LFO recurring interruptions are the fundamental cause of system instability and dependability. Data from the past shows that the employment of stabilizers in power systems has resulted in a reduction in low-frequency oscillations, and that long-term stability has steadily improved with the passage of time. In power system stabilizer we optimize the parameter of lead-lag type PSS for a robust power system using TSA and EO. Specifically, we investigate the performance of two separate systems, one with four machines on a 11-bus system and the other with ten machines on a 39-bus system. By optimizing the parameter of the TSA-based PSS and the EO-based PSS demonstrate the robustness and effectiveness of the two power network systems. The comparison of the simulation findings with other established optimization technique like particle swarm optimization (PSO) shows that TSA and EO are more efficient and robust. According to the simulation findings, the TSA and EO technique decreases the settling time and maximum overshoot more significantly than the other choices.

TABLE OF CONTENTS

LIST OF TABLES

LIST OF FIGURES

LIST OF ABBREVIATIONS

PSS	Power System Stabilizer
TSA	Tunicate Swarm Algorithm
EO	Equilibrium Optimizer
LFO	Low Frequency Oscillations
CPSS	Conventional Power System Stabilizer
PSO	Particle Swarm Optimization
SMIB	Single Machine Infinite Bus
MMN	Multi-Machine Networks
MATLAB	MATrix LABoratory

CHAPTER 1

INTRODUCTION

1.1 Introduction

Despite being the most intricate and biggest networks ever established by mankind, power generating and distribution networks are always prone to a variety of disturbances, the majority of which cause low frequency oscillations (LFOs) between 0.2 and 3.0 Hz [1]. LFOs must be avoided in order to offer the most efficient power transmission and maintain the highest level of power system dependability. Large interconnected power systems exhibit three distinct forms of oscillations: inter-unit oscillations (1–3 Hz), local mode oscillations (0.7–2 Hz), and inter-area oscillations (0.7–2 Hz). Inter-unit oscillations are the most prevalent oscillation type in big interconnected power networks (0.5 Hz) [2]. Once they began, they were likely to continue for an extended period of time. Depending on the circumstances, they may continue to grow, leading to system separation if insufficient damping is provided to compensate. Incorporating power system stabilizers (PSS) into generators allows for the mitigation of system damping. These stabilizers send extra stabilizing feedback signals to the excitation system, therefore reducing system damping. Despite the promise of contemporary control techniques and a variety of structural options, electric power system utilities continue to choose the traditional lead-lag Power System Stabilizer (CPSS) structure over the alternatives now available. Possible causes for this occurrence include the simplicity of online modification and the lack of confidence in the stability of certain adaptive or variable structure approaches [3]. Incorporating modernized automatic voltage regulators and PSS into a power system that utilizes renewable energy sources can aid in enhancing the system's reliability [1].

A linearized model of the power system is used to derive the features of traditional power system stabilizers, which are the most often employed stabilizers (CPSSs). PSSs must be designed in the frequency domain and then implemented using lead-lag compensators, which is achieved by use phase compensation techniques. The CPSS settings must be fine-tuned in response to both types of oscillations in order to provide efficient damping effects throughout a broad operating range. Because power systems are highly nonlinear systems with changing configurations and characteristics over time, it is not possible to guarantee the operation of the CPSS based on a linearized model of the power system in a highly dynamic operating environment [4]. Gibbard [5] demonstrated the effectiveness of CPSS damping over a wide range of system loading situations in his research [3].

In this paper, a robust approach based on the tunicate swarm algorithm (TSA) and Equilibrium Optimizer (EO) provided for the aim of changing the PSS parameters. A large number of machines are investigated in this case study of an electric power system. A multi-machine energy system's dynamic stability is greatly improved as a result of the simulations, according to the findings.

1.2 Background

Developed in response to power system operations on the Pacific Intertie, the Power System Stabilizer (PSS) was originally known as Supplementary Control Systems when it was first introduced in the mid-1960s. Known as inter-area modes of operation, these oscillations occur at extremely low frequencies (less than one hertz), are very lightly damped, and occur at extremely low frequencies. Due to the fact that genuine power oscillations were recorded between the Pacific Northwest and the Southwest, it is referred to as an inter-area phenomenon. In the oscillations, a large number of machines located in one part of the system (the northwest) swinging against machines located in another section of the system (the southeast) (Southwest). When electrical systems were interconnected and electricity was transported from one region to another, the stability margins were lowered gradually, resulting in the development of this predicament. Because of the advent and widespread use of high gain, quick acting excitation devices for system transient stability, inter-area oscillations have become more noticeable in recent years.

Generators are outfitted with stabilizers for the electrical power system networks in order to increase their reliability. If a failure occurs in the power system, the generators will experience fluctuations and lose synchronism. When there is a disruption, the power system becomes unstable.

When power system stabilization (PSS) was developed, it allowed system operators, generator operators, and planners to use the PSS to minimize actual power oscillations by swiftly altering the field of the generator to dampen the low frequency oscillations. The Tunicate Swarm Algorithm (TSA) and the Equilibrium Optimizer (EO) are two distinct optimization strategies that are utilized to stabilize the system. The proposed TSA and EO technique has the potential to successfully tweak the settings of the PSS in order to maintain stability.

In recent years, other traditional CPSS design methods have been detailed, including sensitivity to eigenvalues, phase correction, and the root locus method, to name a few. Traditional procedures take a long time to finish since they are iterative, require a large amount of computing, and produce slow convergence. It's also possible that the PSS settings established via the old method aren't the best [6].

In recent years, intelligent ways for tweaking the parameters of PSS have increased in popularity and have been widely used in place of conventional fixed gain PSS, which has become more rare. Several techniques, including differential evolution [7], genetic algorithm [8], artificial bee colony [6], simulated annealing [9], and other hybrid approaches [10], are being applied to optimize the parameters of PSS for both single machine infinite bus (SMIB) and multi-machine networks [1].

The Tunicate Swarm Algorithm (TSA) is a metaheuristic algorithm inspired by nature. The tunicate's jet propulsion and swarm behaviour had a huge impact on the development of this technology. TSA's overall performance on seventy-four distinct benchmark test issues may be evaluated using ANOVA. Other tests, such as sensitivity, convergence, and scalability, are performed in addition to the ANOVA test. It's also compared to a few well-known metaheuristic tactics that are based on previously discovered optimal solutions. TSA is more successful than its rivals in generating global optimal solutions with greater convergence, according to statistical data. Simulation findings show that TSA gives superior optimum solutions when compared to other competing algorithms [11].

This paper introduces the Equilibrium Optimizer (EO), an unique optimization approach. Control volume mass balance models, which are used to anticipate both dynamic and equilibrium states, inspired the method. Each particle (solution) and its concentration (position) acts as a search agent for other particles in EO (solutions). In order to obtain the equilibrium state, the search agents must update their concentration in respect to the best-so-far solutions, known as equilibrium candidates (optimal result). It has been shown that adopting a well-defined "generation rate" term can improve EO's exploration, exploitation, and avoidance of local minima capabilities. The proposed method is put to the test on 58 unimodal, multimodal, and composition functions, as well as three engineering difficulties. The outcomes are promising. The EO algorithm's architecture includes a lot of exploratory and exploitative search methods, allowing solutions to be altered on the fly. They approach the problem as if it were a black box with input and output states, giving them the benefit of potentially being a future candidate for a user-friendly optimizer [12].

1.3 Power System Stability: Introductory Concepts

Many CIGRE and IEEE articles have addressed power system stability, its classification, and difficulties related with it. The IEEE power systems dynamic performance committee and the CIGRE study committee define power system stability as:

"The capacity of an electrical power system to return its state of operational equilibrium after being subjected to a physical disturbance, with the system variables constrained, such that the entire system stays intact and the service is uninterrupted, is known as power system stability." [13].

The **Fig. 1.1** below gives the overall picture of the stability problem and its solution. In the following, we will discuss the stability problem in more detail. The stability problem can be divided into two parts.

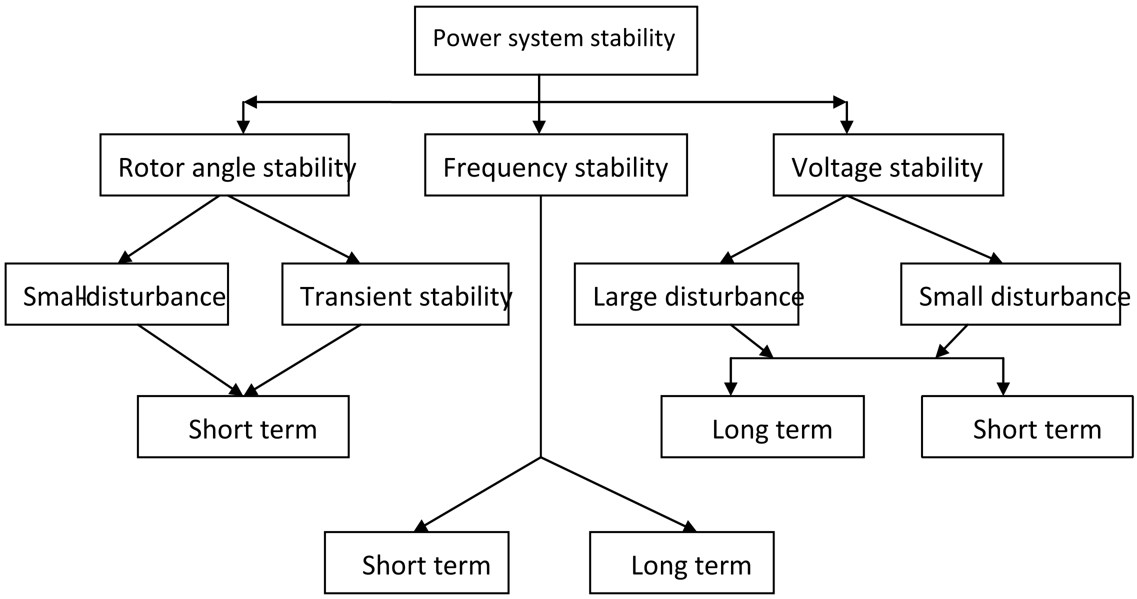

Fig. 1.1 Power-system stability classification [14]

Small disturbance stability, which is a portion of rotor angle stability, is our specific focus in this study. Voltage stability is also addressed in the event of minor interruptions.

1.3.1 Steady-state Stability: The reaction of a synchronous machine to a progressively rising load is referred to as steady-state stability. It is primarily concerned with determining the upper limit of machine loading without losing synchronization, assuming that the loading is steadily raised [15].

1.3.2 Dynamic Stability: The reaction to tiny shocks on the system, which cause oscillations, is called dynamic stability. If these oscillations do not exceed a specific amplitude and fade out fast, the system is considered to be dynamically stable. The system is dynamically unstable if these oscillations continue to develop in magnitude. An interconnection between control systems is frequently the source of this form of instability.

1.3.3 Transient Stability: The reaction to major disturbances, which can cause significant changes in rotor speeds, power angles, and power transfers, is known as transient stability. Transient stability is a brief phenomena that occurs every few seconds. Rotor stability analysis is the most important aspect of power system stability. Various assumptions are required for this, including:

- Balanced three-phase systems and balanced disturbances are evaluated for stability analysis.
- Machine frequency deviations from synchronous frequency are minor.
- Dc offset and high frequency current are present during a generator short circuit. However, theses are ignored while analyzing stability.
- The network and impedance loads have stabilized. As a result, the power flow equation can be used to calculate voltages, currents, and powers [15].

1.3.4 Rotor angle stability

This refers to a synchronous generator's capacity to maintain synchronism despite being subjected to disturbances in an interconnected power system. It depends on the machine's ability to keep the electromagnetic and mechanical torques of each synchronous machine in the system in balance [16]. This type of instability manifests itself as swings in the generator rotor, resulting in synchronism loss.

1.3.5 Small Disturbance Stability

Small disturbance stability might relate to rotor angle stability or small disturbance voltage stability. The disturbances are mild enough that a linearized system model may be assumed. Small disruptions might include gradual load adjustments, control alterations, and so on. Disturbances caused by faults or short circuits are not included [17].

1.4 Objective

Details of our thesis objectives are provided below :

1. To optimize parameters of PSS for stability improvement in multi-machine power system.
2. To investigate better optimization algorithms such as TSA and EO for multi-machine power system.
3. To compare the performance of proposed algorithm with the traditional PSS and PSO based PSS.

1.5 Thesis Layout

The thesis is organized by six different chapters. Detailed information discusses in the chapters.

- **Chapter 1 (Introduction) :** Provides a general introduction, background, and objectives of this study.
- **Chapter 2 (Literature Review)** : In this chapter discuss about literature review on PSS, multi-machine, Classical Control Approaches for Multi-Machine Power System and optimization algorithms.
- **Chapter 3 (Optimization) :** Gives a brief description of two optimization algorithm tunicate swarm algorithm and equilibrium optimizer.
- **Chapter 4 (Methodology) :** In this chapter discuss about the experimental work and methodology with two examples.
- **Chapter 5 (Results and Discussion) :** Presents analysis of the results obtained and comparison between two algorithms.
- **Chapter 6 (Conclusion) :** Provides the summary according to the finding of this study. In addition, some limitations and suggestion for future researchers also discuss there.

CHAPTER 2

LITERATURE REVIEW

2.1 Introduction

The ability of an electrical power system to return its state of operating equilibrium after being subjected to a physical disturbance, with the system variables bounded, such that the entire system stays intact and the service remains uninterrupted, is known as power system stability. Intelligent methods for modifying PSS parameters have grown in popularity in recent years, and are now frequently employed in favour of traditional fixed gain PSS, which has become increasingly rare.

In this chapter, we discussed about some linear control approaches in multi-machine power system and robust control approaches in multi-machine power system. Here presented a tabular form of multi-machine stability related information of some researcher.

2.2 Literature review on PSS:

In this paper [18], A.E. Leona, J.M. Mauricio, and J.A. Solsona show how to make a nonlinear observer-based excitation controller. The controller only needs to know the current and speed of the rotor. It does not need to know the load angle. The problem with this paper is that the FACTS devices are not all put together. Ramesh Devarapalli. Biplab Bhattacharya. Nikhil Kumar Sinha. Amended GWO algorithms were made by Bishwajit Dey [19]. Amended GWO is used to improve traditional PSS. But it hasn't been proven by experiments. Also, no sources that can be reused are used. In this research, TCSC and PSS have been put together by G. Shahgholian, A. Movahedi, and J. Faiz [20]. It is a strong design because the PSO Algorithm is used to tune the parameters of PSS and TCSC. There are some problems, like the fact that no renewable sources are thought about and tested on a single network. [21] In this research, H. Shayeghi, A. Safari, and H. A. Shayanfar coordinated PSS and TCSC, and they used two different algorithms to find the best values for the parameters: Velocity update relaxation particle swarm optimization (VURPSO) and the Genetic algorithm (GA). But the best place to put the controller isn't talked about, and no renewable sources are taken into account. A. B. Khormizi and A. S. Nia [22] designed a method for coordinating the design of the PSS and TCSC using a genetic algorithm. The best place to put the controller was also figured out. There are some limits, like the fact that no FACTS devices are used and no online tuning has been done.

2.3 Literature Review on Multi-Machine

A paper published in 2012 by E. Nechadi, M. N. Harmas, A. Hamzaoui, and N. Essounboul compared the performance improvements achieved by three different controllers, including better oscillation damping, faster transient dynamic behavior, and better transient dynamic behavior over three different controllers. They made use of single-machine infinite-buses as well as multi-machine parallel processing systems [23]. Using a simulation on the Western System Coordinating Council system, H. Huerta, A. G. Loukianov, and J. M. Caedo demonstrate in their research that the controller was evaluated and compared to a traditional one. They published their findings in 2009. They employed nine buses, three generators, and three loads from the Western System Coordinating Council (WSCC) to conduct the test [24]. In the year 2013, the work of A. Ghasemi, H. Shayeghi, and H. Alkhatib is demonstrated. The controller's minimal performance needs have been identified, and this performance has been reached by employing the FGSA method of optimization. The test networks consist of a three-machine 9-bus system and a ten-machine 39-bus system [2]. H. E. Psillakis and A. T. Alexandridis published a paper in 2005 shows Theoretical findings are demonstrated that serve as the framework for the construction of a controller of this type, and simulation results support our theoretical conclusions by demonstrating that the system performs quite satisfactorily. The test network is a two-generator infinite bus power system with a total of eight generators [25]. In the year 2000, R. Mahanty and P. Gupta conducted a study in which they examined The results demonstrate that the suggested TS-based strategy, regardless of the original solution, ultimately leads to the best solution in the end. As an illustration of their research, they used 3-machine 9-bus and 10-machine 39-bus [26]. Using an NSGAII-based PSS, T. Guesmi, A. Farah, H. H. Abdallah, and A. Ouali suggested that the system electromechanical modes at different loading circumstances and system configurations be shifted as much as feasible concurrently in a pre-specified zone, namely the D-shape sector, in 2017.As an illustration, they utilized a 3-machine 9-bus power system and a 10-machine 39-bus power system [27]. Researchers M. A. Mahmud, M. J. Hossain, H. R. Pota, and A. M. T. Oo demonstrate in their work conducted in the year 2017 Designing a robust controller by partial feedback linearization while taking into account two-axis models of synchronous generators is accomplished, and modeling the uncertainties within power system models is accomplished based on the fulfilment of matching requirements. In order to demonstrate their point, they employed an IEEE 39-bus, 10-machine benchmark power system [28]. In 2016, Z. Bouchama, N. Essounbouli, M. N. Harmas, A. Hamzaoui, and K. Saoudi published an analysis showing that the removal of transient modes decreases convergence time while simultaneously boosting robustness. Chattering is eliminated by using a continuous control rule. dependence on things that are not quantifiable As a test network, a three-machine, nine-bus power system was used for the analysis [29]. In 2012, V. Pant, B. Das, and A. Bhargava conducted an investigation into the development of a linearized model of a multi-machine power system utilizing STATCOM. As a test network, the 39-bus, 10-machine New England power system was used for the analysis [30]. In 2012, research by R. Hemmati, M. Nikzad, and S. S. S. Farahani demonstrates The simulation results indicated that resilient approaches are capable of controlling a power system in the presence of uncertainty. As a test network, they deployed a 2-area, 4-machine power system with one uninterruptible power supply (UPFC) [31]. When S. Shojaeian, J. Soltani, and G. Arab Markadeh published their study in 2012 on the simulation results produced using PID controllers, they demonstrated that these controllers were not capable of dampening the low frequency oscillations of the faulty power system under discussion. The IEEE 30-bus system, two-area, and four-machine power system network were employed to replicate the situation [32]. A study conducted by K. Saoudi and M. N. Harmas, published in 2014, demonstrated that the proposed approach is effective and robust in damping local and inter-area modes oscillations while simultaneously improving system stability significantly when compared to other power system stabilizers that have been considered. They conducted their investigation using a two-area, four-machine power system network in 2016 [33]. In their research, R. K. Patnaik and P. K. Dash find that the back-stepping controller, the DFIG, is very effective at improving (damping) the inter-area oscillations of a conventional two-area, four-machine network (embedded with the PSS), as shown in the simulation and results section. In their simulation, they used a two-area, four-machine system with a DFIG-based wind farm [34]. Journal of Electrical and Electronics Engineering (2015) published a research in which wide-area remote control signals were incorporated as the feedback signal for each FACTS damping controller, resulting in improved coverage of the inter-area oscillations. It was necessary to calculate and compare the modal residues of several feedback signal candidates to system inputs in order to make an appropriate selection of the feedback signals. A five-area, sixteen-generator, 68-bus system is employed for the testing [35]. A sliding mode control technique for stabilizing multimachine power systems utilizing just static output feedback is demonstrated by X G Yan, C Edwards, S K Spurgeon, and J. A. M. Bleijs in their 2004 publication. A composite sliding surface is first created using the approach given by Edwards and Spurgeon. A three-machine power system network is then employed for the testing [36].

2.4 Literature Review on Classical Control Approaches for Multi-Machine Power System

Z. Jiang had published their paper in 2008 and used Single machine-infinite bus system and as a controller they used synergetic control synthesis and the synergetic control theory was then used to come up with a nonlinear control law. Check out how well the proposed PSS works [4]. T. K. Roy, M. A. Mahmud, W. Shen, and A. M. T. Oo published a work in 2016 using a 2-area, 4-machine, 11-bus power system and non-linear adaptive backstepping coordinated controller. The developed control technique maintains multimachine transient stability better than NCC and ECSMC [37]. Partially evaluating M. A. Mahmud, H. R. Pota, M. Aldeen, and M. J. Hossain found shorter settling time, damped oscillations, and reduced steady-state error using their linearizing excitation controller and 2-area, 3-machine 11-bus system in 2014 [38]. In 2017, a paper was published by T. Fetouh and M. S. Zaky and they used coordinated SVC-PSS stabilizer controller, and 3 machine, 9-bus power system. As its successfully minimized the computational time as well as the storage capacity [39]. SSEC controller and New England 10-generator 39-bus power system is used in a research by H. Kang, Y. Liu, Q. H. Wu, and X. Zhou in 2015, and we can see the SSEC is capable of enhancing both the rotor angle stability and the voltage stability of the power system damps oscillations under severe disturbance conditions [40]. Another paper used 2-area, 4-machine power system, IEEJ West 10-machine system, SMIB power system and its showed two different controlling errors are minimized by updating the parameters in online mode, also its used online trained self-recurrent wavelet NN controller, discrete Lyapunov theory which was published by M. Farahani in 2012 [41]. In 2012, P. He, F. Wen, G. Ledwich, Y. Xue, and K. Wang published their paper where they used CPSS, SNPSS, APSS,MBPSS controller which improved damping ratios of most electromechanical modes and 8-unit 24-bus power system had been used. The effectiveness of the proposed scheme has been validated on two test systems [42]. Heffron-Phillip's model and linearized dynamic model was used in a research by F. M. Hughes in 2010 and they also used single machine infinite bus.its demonstrated that steady-state voltage stability index and the time domain simulation results verify effectiveness of the proposed method [43]. In 2015, H. Hasanvand, M. R. Arvan, B. Mozafari, and T. Amraee published their paper and used HSVs, RHP-zeros, POD, POD-TCSC & PSS controller and 16-machine 68-bus test system had been used. We can see large number of iterations required by the grid-search algorithm, and it gives satisfactory robust performance [44]. S. Hameed, B. Das, and V. Pant published their paper in 2010, as a controller they used STFPIC and 2-area 4-machine power system and 10-machine 39-bus system had been used. The effectiveness of the proposed scheme has been validated on two test systems [45]. In 2007, J. Zhang, J. Y. Wen, S. J. Cheng, S. Member, and J. Ma published their paper using New England 39-bus test system and SVC controller also we can see steady-state voltage stability index and the time domain simulation results verify effectiveness of the proposed method [46]. H. Zhao, X. Lan, N. Xue, and B. Wang was published their paper in 2013 and the investigated that EGBR technique is used to reduce numerical calculating time of the excitation predictive control and they used Balanced Reduced Model also used four machine power sytem [47]. Optimal solution based on GASA controller used in a paper published by H. Liu, X. Xie, L. Wang, and Y. Han in 2015 and they used One-line diagram of the equivalent transmission system and All possible operating conditions of the system are .covered [48]. In 2010, M. Zarghami, M. L. Crow, J. Sarangapani, Y. Liu, and S. Atcitty investigated that specifies the bus voltages (phase and magnitude) at the sending and receiving ends of the UPFCs to damp the oscillations, results of this controller are compared with and without ECs. As controller they used UPFC and also used 118-bus IEEE test system [49]. Single-machine infinite-bus multi-machine systems and MJLS, PSS controller used in a paper in 2015 by H. Soliman and M. Shafiq and as contribution of the paper we can see it achieves robust stochastic stability as well as regional pole placement [50]. Minimum cut methodology and IEEE 6-bus, IEEE 30-bus and IEEE 118-bus systems used in a paper in 2014 by T. Duong, Y. Jiangang, and V. Truong and it finding the location, quantity and size of TCSC [51]. In 2009, F. C. Jusan, S. Gomes, and G. N. Taranto published their paper and used dynamic phasor model of SVC, Modal analysis and as bus system they used the system-2 of the IEEE-2nd Benchmark Model. Demonstrated that effectiveness of the controller was confirmed through linear and non-linear time domain simulations and suitable for high frequency analysis [52].

2.5 Literature review on optimization algorithms

Complex optimization problems are solved by introducing a number of algorithms. The genetic algorithm (GA) [53] is one of the most famous evolutionary algorithms. Charles Darwin's theory of evolution inspired this algorithm. In reality, GA is based on the idea that the strongest survive. In nature, fitter animals have a better chance of staying alive. Particle Swarm Optimization is the most common swarm-based algorithm (PSO) [54]. The PSO algorithm is based on how birds move together in nature. In this approach, each particle is treated as a solution to a specific optimization problem. The Grey Wolf Optimizer (GWO) [55] is based on how grey wolves find food and make decisions about who should lead them. The hierarchical system is imitated by using four types of grey wolves: alpha, beta, delta, and omega. Also, the optimization includes three important foraging steps: searching for prey, approaching prey, and killing prey. This paper [56] describes the Whale Optimization Algorithm (WOA). This method uses three operators to mimic how humpback whales look for food, circle it, and catch it in a bubble net. In this paper [57], the Dragonfly algorithm is suggested for solving single-objective and multiple-objective problems. It imitates the static and dynamic behaviors of dragonflies for swarm intelligence algorithms' ability to explore and exploit. This paper proposes a new meta-heuristic algorithm called Jellyfish Search (JS) optimizer [58]. It is based on how Jellyfish look for food in the ocean. Jellyfish's active and passive movement is used to model exploration and exploitation.

CHAPTER 3

OPTIMIZATION

3.1 Introduction

In this chapter, we discuss about two novel optimization algorithms called tunicate swarm optimization and equilibrium optimizer. This two algorithms Inspiration are discuss in first. The proposed algorithm's inspiration and mathematical modeling are discuss in detail. Also the working principle of this two algorithms are described.

An optimization algorithm is a method for comparing multiple solutions iteratively until the best or most satisfying one is found. Optimization has become a feature of computer-aided design activities since the invention of computers. Nowadays, there are two types of optimization algorithms that are commonly used.

3.2 Tunicate Swarm Optimization

Tunicate Swarm Algorithm (TSA) is a bio-inspired metaheuristic algorithm for solving non-linear constrained problems. Its deep-sea activity was inspired by tunicate swarms. This work's contributions are:

• TSA, a bio-inspired tunicate swarm algorithm, was proposed. Swarm behavior and tunicate jet propulsion are both modeled.

• 74 benchmark test functions are used to test the proposed TSA.

• State-of-the-art metaheuristics are compared to the TSA algorithm.

• The TSA algorithm's design problem-solving efficiency is investigated.

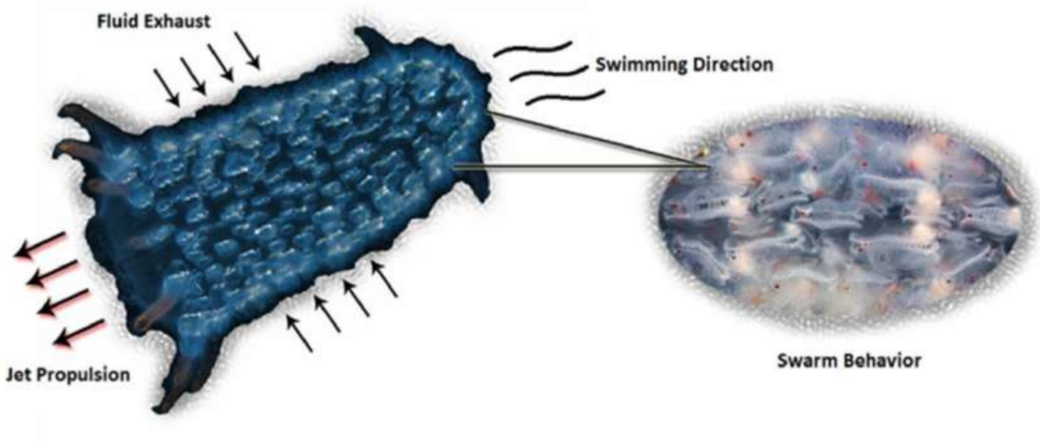

Fig. 3.1 Tunicate swarm in deep ocean [11]

3.2.1 Inspiration

Tunicates are bioluminescent, emitting a soft blue–green light that may be seen from several meters away. Tunicates are cylinder-shaped clothing having one open and one closed end. [59]. The tunicate is tiny. A gelatinous tunic connects each tunicate. Each tunicate takes water from the sea and creates jet propulsion using atrial siphons. Tunicate is the only mammal with fluid jet propulsion. This propulsion helps tunicates swim vertically. Tunicates live 500–800 meters deep and move to the surface at night. Tunicates range from millimeters to 4 meters [60]. The most interesting fact of tunicate is their jet propulsion and swarm behaviors (see **Fig. 2**), which is the main motivation behind this paper.

3.2.2 Motivation

Both business and academics have been paying close attention to nature-inspired algorithms over the last few decades. As a result of this, academics have developed a number of algorithms based on natural inspiration. The bulk of algorithms in the catalog of suggested nature-inspired techniques are biology or bio-inspired since they are based on the concept of certain biological system features. Swarm intelligence has inspired a unique class of bio-inspired algorithms. Because of their capacity to exhaustively explore the search space and return the global optima, population or multiple-solution based swarm intelligence algorithms are capable of addressing a wide range of real-world optimization issues. The No Free Lunch theorem also states that these techniques cannot solve all optimization issues [61]. This inspired us to develop a novel population-based metaheuristic approach to handle many optimization issues.

3.2.3 Tunicate swarm algorithm (TSA)

In this part, the motivation and mathematical modeling of the suggested approach are discussed.

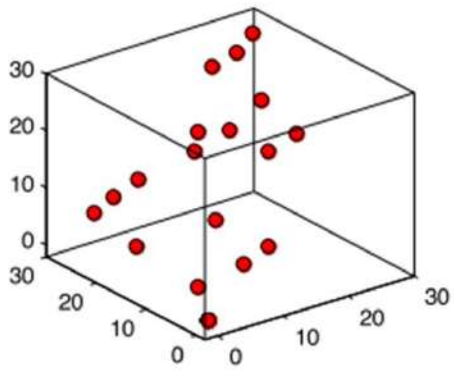

Fig. 3.2 Searcher conflict avoidance [11]

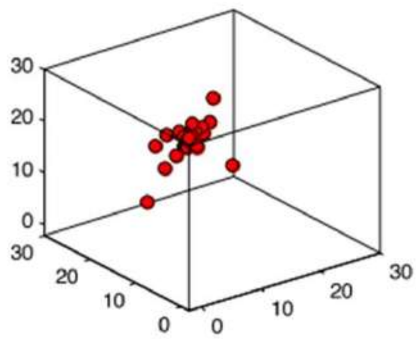

Fig. 3.3 Searching for the perfect neighbor [11]

3.2.4 Mathematical model and optimization algorithm

Tunicate can find aquatic food. The search space provides no food source information. Two tunicate behaviors are utilized to pick the appropriate food source. These include jet propulsion and swarm intelligence. A tunicate must prevent conflicts between search agents, move toward the optimal search agent's position, and stay close it to mathematically approximate jet propulsion behavior. Swarm behavior updates other search agents on the best option. Following subsections model these phenomena mathematically.

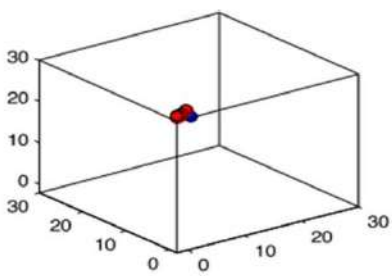

Fig. 3.4 Aim for top search agent [11]

3.2.4.1 Search agent conflicts

To prevent conflicts between search agents , vector A is used to calculate new search agent position, as illustrated in **Fig. 3.2**.

$$\vec{A} = \vec{G}\vec{M} \tag{1}$$

$$\vec{G} = c2 + c3 - \vec{F} \tag{2}$$

$$\vec{F} = 2 \cdot c1 \tag{3}$$

However, $\vec{G}$ is the gravity force and $\vec{F}$ shows the water flow advection in deep ocean. The variables $c1$, $c2$, and $c3$ are random numbers lie in the range of [0, 1]. $\vec{M}$ represents the social forces between search agents. The vector $\vec{M}$ is calculated as follows:

$$\vec{M} = [P_{min} + c1 \cdot P_{max} - P_{min}] \tag{4}$$

where P_{min} and P_{max} denote social interaction speeds. Pmin and Pmax are 1 and 4 in this work.

3.2.4.2 *Best-neighbor movement*

After avoiding neighbor disagreement, search agents proceed to best neighbor (see **Fig. 3.3**).

$$\vec{PD} = | \vec{FS} - rand \cdot \vec{P}p(x) | \tag{5}$$

P D is the distance between the food source and tunicate, x is the current iteration, and F S is the ideal food source location. P p (x) represents tunicate location and rand is a random number [0, 1].

3.2.4.3 *Best search agent*

The best search agent (i.e., food source) is depicted in **Fig. 3.4**.

$$P_P(x) = \begin{cases} FS + A.PD, & if\ r_{and} \geq .5 \\ FS - A.PD, & if\ r_{and} \leq 0 \end{cases} \tag{6}$$

where $\vec{P}p(x')$ is the updated position of tunicate with respect to the position of food source $\vec{FS}$.

3.2.4.4 Behavior of swarms

To mathematically simulate tunicate's swarm behavior, the top two best solutions are kept and other search agents' placements are updated based on their locations. Formula for tunicate swarm behavior:

$$P\vec{\ }p\,(x + 1) = P\vec{\ }p\,(x) + P\vec{\ }p\,(x + 1)\ 2 + c1 \qquad (7)$$

Fig. 3.5 depicts how search agents update based on P p (x). The ultimate location is arbitrary inside a cylindrical or cone-shaped tunicate. Algorithm shows the TSA's pseudocode. TSA algorithm highlights include:

- A, G, and F help solutions act randomly in a search space and prevent agent conflicts.
- Variations in vectors A, G, and F improve exploration and exploitation.
- Tunicate jet propulsion and swarm activity in a specific search space defines TSA algorithm's collective behavior (see **Fig. 3.6**).

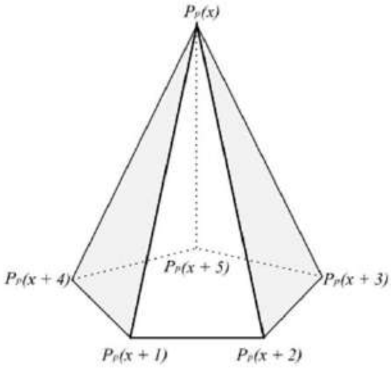

Fig. 3.5 Tunicate 3D vectors [11]

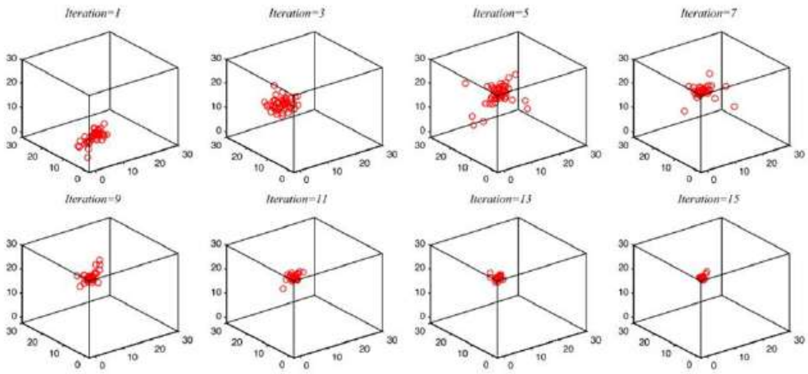

Fig. 3.6 Two-dimensional tunicate jet propulsion and swarming [11]

3.2.4.5 Steps and flowchart of TSA

The following provides an outline of the TSA, including its individual procedures as well as its flowchart (see **Fig. 3.7**).

Step 1: Initialize the tunicate population $P^{\rightarrow}$.

Step 2: Choose the initial parameters and maximum number of iterations.

Step 3: Calculate the fitness value of each search agent.

Step 4: After calculating the fitness value, the best search agent in the given search space is investigated.

Step 5: Using equations, update the position of each search agent.

Step 6: Fine-tune the revised search agent to travel outside the search space's border.

Step 7: Calculate the revised fitness value of the search agent. Update if a better option exists than the prior optimal solution.

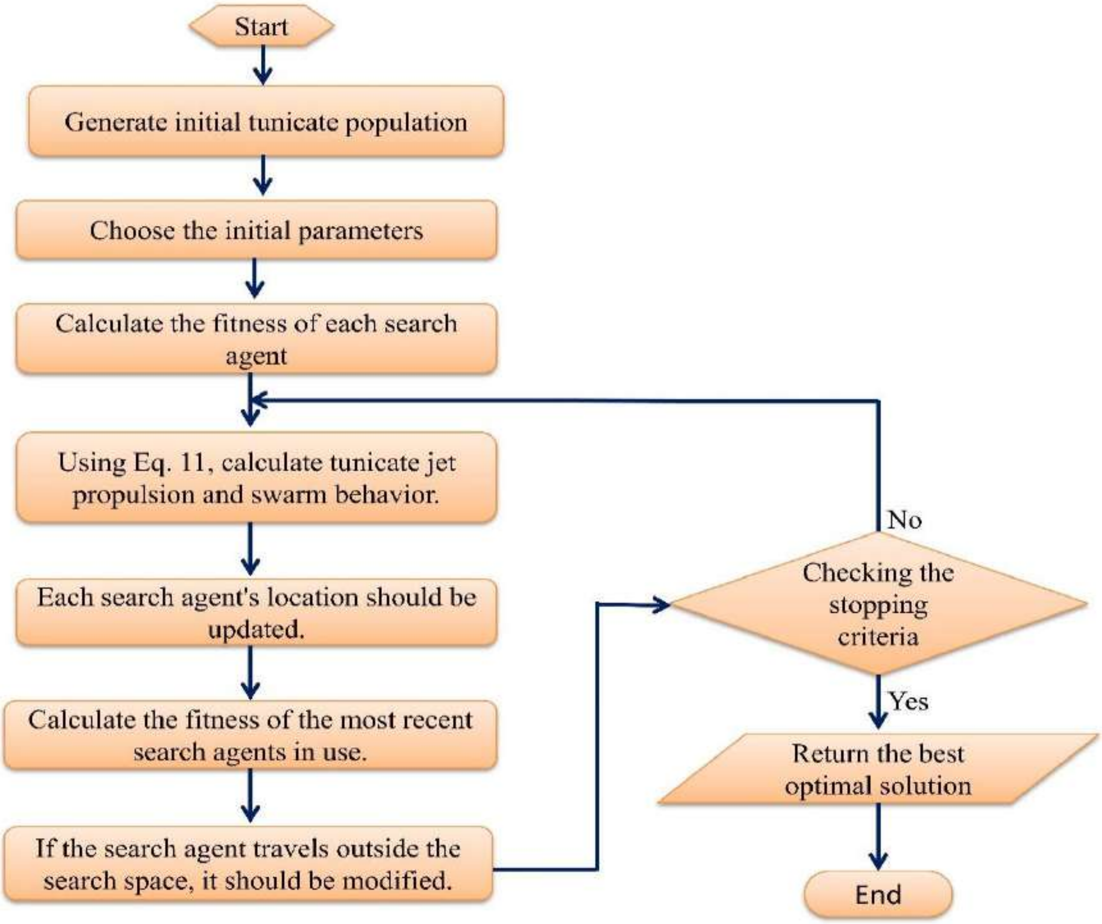

Fig. 3.7 Flowchart of tunicate swarm optimization

3.3 Equilibrium Optimizer

The Equilibrium Optimizer (EO) is a novel optimization approach influenced by control volume mass balance models. Each particle (solution) works as a search agent in EO (position). Search agents update their concentration randomly on best-so-far solutions, called equilibrium candidates, to reach equilibrium (optimal result). EO's ability to explore, exploit, and avoid local minima is improved with a well-defined "generation rate" term. The suggested technique is tested using three engineering application problems and 58 unimodal, multimodal, and composition functions.

3.3.1 Inspiration

The EO approach uses a well-mixed dynamic mass balance on a control volume to describe the concentration of a nonreactive substance as a function of its numerous source and sink processes. Mass balancing equation conserves mass entering, departing, and generated in a control volume. Mass-balance equation is a first-order ODE [62], A system whose change in mass over time is equal to the mass entering the system plus the mass created within minus the mass leaving the system is called:

$$V\frac{dC}{dt} = QC_{eq} - QC + G \tag{8}$$

C indicates the equilibrium concentration when there is no mass creation inside the control volume, the rate of mass change in the control volume, and the volumetric flow into and out of the control volume. When, balance is stable. We can solve for as a function of where represents the inverse of the residence time, or turnover rate. Rearranging Equation to find C as a function of t:

$$C = C_{eq1} + (C_o - C_{eq1})F + \frac{G}{\lambda V}(1\text{-}F) \tag{9}$$

Based on the integration interval, first start time and concentration. The equation may be used to determine the concentration in the control volume with a known turnover rate and a specified generation rate. These equations are used to develop EO in this section. A particle in EO is like a solution, and its concentration represents its PSO position. As observed in Eq., a particle's updating rules and concentration are updated by three terms. Equilibrium concentration is one of the best-so-far solutions selected at random from the equilibrium pool. The second phrase refers to a particle's concentration difference from equilibrium, which is a direct search process. This term urges particles to explore the globe. Third, the generation rate functions as an exploiter or solution refiner, especially with small steps, but it may also be an explorer. Each term is defined and how it influences search.

3.3.2 Initialization and function evaluation

EO optimizes the starting population, like other meta-heuristic algorithms. Initial concentrations in the search space are depending on the number of particles and dimensions.

$$C_i^{initial} = C_{min} + Rand_i(C_{min} - C_{max}); \;\; i = 1,2, \ldots \ldots n \tag{10}$$

C is the starting concentration vector of the i-th particle, min and max represent the dimensions, Randi is a random vector in [0,1], and n is the population size. After evaluating particles' fitness, equilibrium candidates are sorted.

3.3.3 Candidates and the pool of equilibrium

The equilibrium state of the algorithm is the global optimum. Because the equilibrium point is unknown at the start of the optimisation problem, only equilibrium candidates are employed to construct a particle search pattern. These candidates contain the four best-so-far particles discovered throughout the optimization process, as well as another particle whose concentration is the sample average of the four particles, based on many trials in different case scenarios. Four options improve EO's investigation, while the average improves exploitation. The number of candidates is determined at random and is determined by the optimization problem. The literature advises employing a different number of candidates [63]. GWO uses alpha, beta, and omega wolves to update the positions of other wolves. Using fewer than four candidates reduces the method's performance in multimodal and composition functions while improving unimodal results. Four candidates have backfired. These five particles are equilibrium candidates, and they are used to construct the equilibrium pool vector.

$$C_{eq.pool=} C_{eq1}. C_{eq2}. C_{eq3}. C_{eq4}. C_{eq(ave)} \tag{11}$$

Each particle in each cycle modifies its concentration by randomly picking candidates from a pool of candidates with the same possibility. For example, in the first iteration, the first particle updates all of its concentrations based on; in the second iteration, it may update its concentrations based on. Each particle will continue through the updating process until the optimization process is complete, with all candidate solutions receiving about the same amount of updates.

3.3.4 Exponential term (F)

The exponential element helps update the basic concentration rule (F). A precise definition will help EO balance exploration and exploitation. Since a real control volume's turnover rate varies over time, is considered to be a random vector in [0,1]:

$$\vec{F}=e^{-\vec{\lambda}(t-t_o)} \tag{12}$$

Where time is a function of iteration and decreases with iterations:

$$t \;\; = (1-\frac{Iter}{Max\_iter})^{(a_2\frac{Iter}{Max\_iter})} \tag{13}$$

Where and are the current and maximum iterations, respectively, and is a constant used to regulate exploitation ability. This study explores the following to assure convergence by lowering search speed and enhancing algorithm exploration and exploitation:

$$t_o=\frac{1}{\lambda}In\big(-a_1 sign(r-0.5)\big[1-e^{-\lambda t}\big]\big)+t \tag{14}$$

Which constant controls exploration? More exploration means less exploitation. Higher means better exploitation and lower exploration. Third, exploration and exploitation direction. 0-1 random vector r Throughout this work, and are 2 and 1, respectively. Empirical testing of a subset of test functions selects these constants.

$$F=a_1 sign(r-0.5)\big[1-e^{-\lambda t}\big] \tag{15}$$

3.3.5 Rate of generation (G)

The suggested technique uses the generation rate to improve the exploitation phase and deliver an exact answer. Many engineering applications employ models to express generation rate as a function of time [64]. One multifunctional model that defines generation rates as first-order exponential decay is:

$$G=G_o e^{-k(t-t_o)} \tag{15}$$

G0 is the starting value; k is a decay constant. This study assumes and employs the previously computed exponential term to regulate and systematize the search pattern and restrict random variables. Finally, the generation rate formulae are:

$$G = G_o e^{-k(t-t_o)} = G_o F \tag{16}$$

Equation is used to generate random values in the range [0,1], and the GCP vector is produced. GCP stands for Generation Rate Control Parameter, and it contains the contribution of each generation term to updating. The probability of generation affects how many particles use generation to change their states (GP). Particle-level equations dictate its contribution. G is zero if GCP is 0, and all particle parameters are modified without a generation rate factor. GP = 0.5 balances exploration and exploitation well. EO's updated rule will be:

$$C = C_{eq} + \left(c - C_{eq}\right).F + \frac{G}{\lambda V}(1\text{-}F) \tag{17}$$

Where F and V are variables. First term is concentration equilibrium, second and third terms are concentration variations. The second phrase searches for the best position. This phrase allows for significant concentration swings, enhancing investigation (i.e., a direct difference between an equilibrium and a sample particle). The third phrase provides a point to the response. The generation rate term controls minor concentration changes, hence this term contributes more to exploitation. The second and third components' signs depend on particle concentrations, equilibrium candidates, and turnover rate. Same sign increases variance, which helps with domain-wide searches, whereas opposite sign minimizes variation for local searches. The second term searches answers far from equilibrium possibilities, whereas the third term refines them closer. Small denominator turnover rates (e.g., 0.05) increase variation and assist exploration. Figure 1 shows how these characteristics affect exploration and exploitation. In equation, denotes the second term, and the third (G is the function of G0). Term generators govern these disparities. This huge fluctuation only happens in dimensions with minuscule values because each dimension changes. This capability, comparable to an evolutionary algorithm's mutation operator, helps EO exploit solutions.

3.3.6 Memory saving for particles

Memory-saving techniques help each particle keep track of its spatial coordinates, affecting its fitness. This is like PSO's pbest. The superior fitness value from each iteration is replaced. This technique improves exploitation, but without global exploration, it may lead to local minima [65].

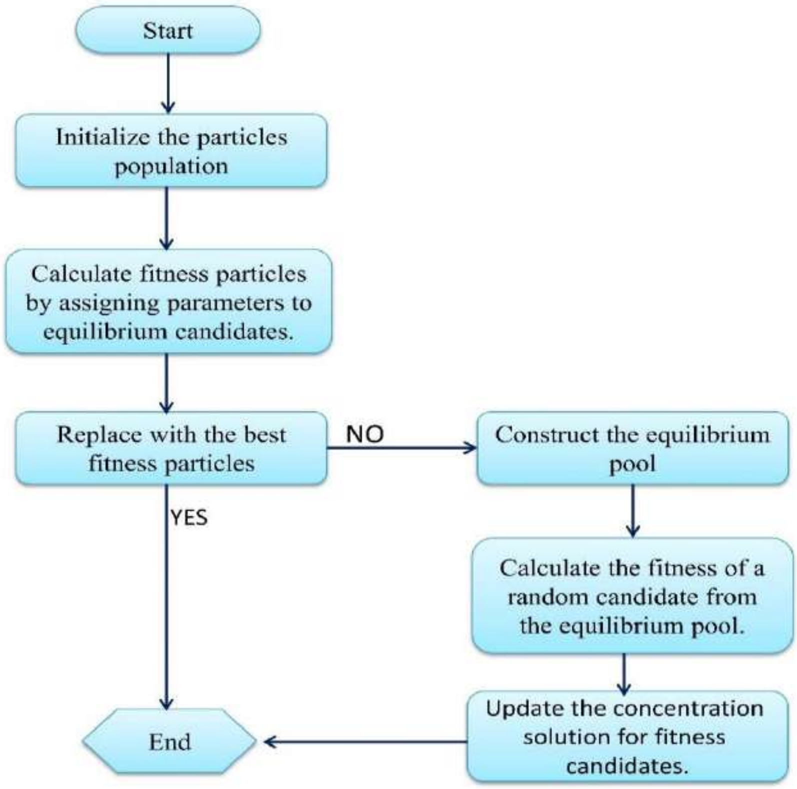

Fig. 3.8 Flowchart of Equilibrium Optimizer (EO)

CHAPTER 4

METHODOLOGY

4.1 Introduction

In this section, we will discuss about power system stabilizer, stability issues, where we used PSS. We also discuss about lead-lag power system stabilizer and synchronization generator which is used in our research as controller. At last, we will deeply discuss about 4-machine 2-area network and IEEE-39 Bus bar system with 10-machine for both tunicate swarm algorithm (TSA) and equilibrium optimizer (EO).

4.2 Power System Stabilizer: An Introduction

4.2.1 Power System Stabilizers (PSS)

The term "power system stabilizer" refers to an electronic control system installed on a generating unit that helps to dampen dynamic oscillations in the power system. The PSS monitors Generator variables such as voltage, current, and shaft speed, then analyses the data and delivers control signals to the voltage regulator [66]. PSS stands for generator control equipment that is utilized in feedback to dampen rotor oscillation produced by tiny disturbances. This disturbance might be generated by even little changes in the automated voltage regulator/reference exciter's voltage, resulting in ever-increasing rotor oscillations. As a result, the PSS helps to improve power system small-signal stability.

4.2.2 Stability Issues and the PSS

The excitation system regulates the system voltage. AVRs are helpful for adjusting generated voltage via excitation control. Extensive usage of AVR affects the power system's dynamic stability or steady state stability because low frequency oscillations (usually 0.2 to 3 Hz) remain in the system and can compromise its power transmission capabilities [67]. The power system stabilizers (PSS) attenuate oscillations by modulating the excitation system, adding system stability [68]. PSS produces damping torque in phase with rotor oscillations by sending a signal to the excitation system.

4.2.3 Design Considerations

PSS can have a significant impact on power system transient stability, despite its primary goal of damping out oscillations. Because PSS dampens oscillations by controlling generator field voltage, the VAR output swings [69]. PSS gain is carefully calibrated to ensure an adequate Volt/VAR swing gain margin. The Wash-Out Filter's time constant may be modified to reduce input signal frequency swing [68]. Large fluctuations in frequency and speed may act through the PSS and cause instability, therefore a control enhancement may be needed during loading/unloading or generation loss. Changing limit logic can lessen these constraints while preserving PSS damping for other system events. PSS interaction with other controls, such as HVDC, SVC, TCSC, and FACTS, may be part of the excitation system or external systems. In addition to low-frequency oscillations, the PSS input includes high-frequency turbine generator oscillations. Before commissioning PSS, the possible PSS-torsional interaction should be studied and verified [68].

4.2.4 PSS Input Signals

Multiple PSS designs exist. Several PSS models were built employing speed, electrical power, and rotor frequency. Below are several [17].

4.2.4.1 Speed as a Input

To minimize rotor oscillations, a power system stabilizer employing shaft speed as an input must produce torque in step with speed changes.

4.2.4.2 Power as a Input

Because of its low-level torsional interaction, accelerating power is a preferred input signal to the PSS. Using a filtered speed signal lowers mechanical power fluctuation. Electrical power feedback typically uses input power.

4.2.4.3 Frequency as a Input

As the external transmission system weakens, the frequency signal's sensitivity to the rotor input rises, counteracting the decline in stabilizer output to electrical torque, as demonstrated by the input signal sensitivity factor concept.

System schematic for the power system stabilizer is presented in the following **Fig. 4.1**.

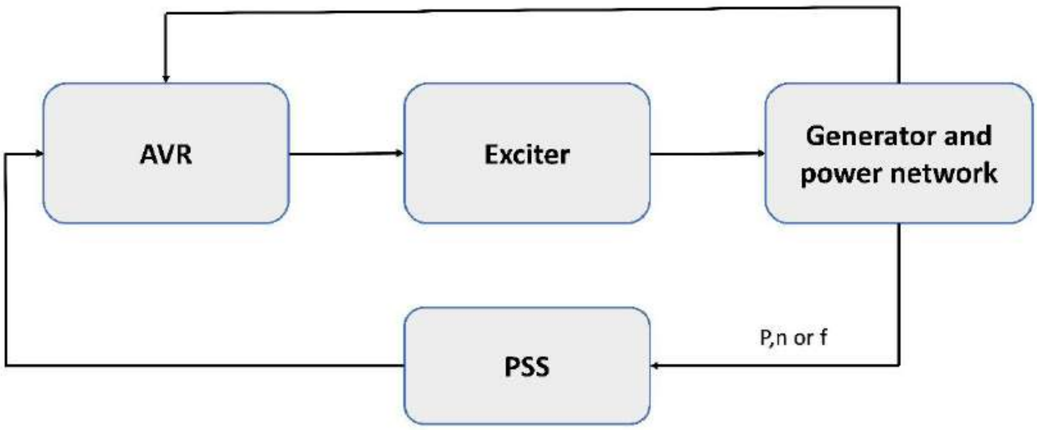

Fig. 4.1 System diagram of PSS

4.3 Lead Lag Power System Stabilizer

A conventional two-stage lead-lag type PSS is depicted in **Fig. 4.2**, with the input and output signals being the change in generator angular frequency ($\Delta\omega_i$) and the control signal (U_{pssi}), respectively. The washout/rest block is used to deactivate the PSSs during steady state operation, and a limiter block is used to reduce the strength of the control signal during transient operation.

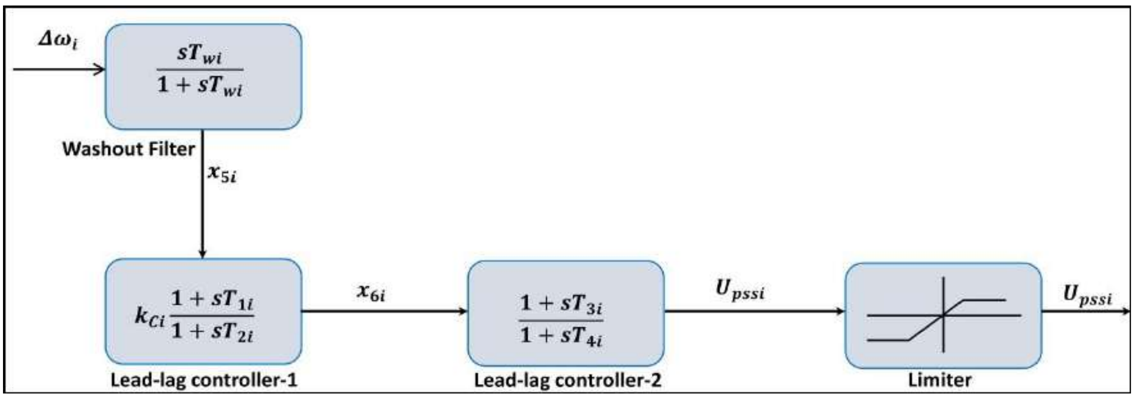

Fig. 4.2 Function block diagram

4.4 Optimization Problem Proposed

Engineers build power systems with the goal of improving the damping of the system by optimizing the goal function (J), as shown below.

$$J = Max\zeta_i \; \{ i = 1,2,3, \dots, n\} \tag{18}$$

ζ is the lowest electromechanical damping ratio, and n is the total number of machines. How to generate a lead-lag PSS design optimization issue in the framework:

Maximize *J*

Subject to:

$$K_{ci}^{min} \le K_{ci} \le K_{ci}^{max}$$
$$T_{1i}^{min} \le T_{1i} \le T_{1i}^{max}$$
$$T_{2i}^{min} \le T_{2i} \le T_{2i}^{max}$$
$$T_{3i}^{min} \le T_{3i} \le T_{3i}^{max}$$
$$T_{4i}^{min} \le T_{4i} \le T_{4i}^{max}$$

4.5 Synchronous Generator

Synchronous generators have the same rotor speed as the stator's magnetic field. Structure-wise, it's divided into revolving armature and spinning magnetic field.

Synchronous alternators are prevalent. Hydropower, thermal power, nuclear power, and diesel power all utilize it.

External characteristics of a synchronous generator are the curve of terminal voltage change when load current changes under constant internal potential. The test measures the generator's internal impedance or vertical axis synchronous reactance. It's a synchronous generator with a load indication. Synchronous generators employ thyristor rapid excitation and damper windings, and the vertical axis synchronous reactance is transient, not steady state.

Due to the controlling influence of the excitation system, exterior properties can be intentionally generated. Positive external characteristic: terminal voltage lowers as load current increases; negative: terminal voltage increases. Overall excitation can be altered by 15%.

Since synchronous generators use DC excitation, the voltage may be readily changed by adjusting the excitation current while each machine operates individually. After being connected to the grid, the voltage can't be changed. Changing the excitation current adjusts the motor's power factor and reactive power.

Synchronous generators have no-load and load characteristics. These qualities help users choose generators. (more information in **Fig. 4.3**).

The following equations show that a network of n generators may be represented as a fourth-order dynamic system [13]-[70]. Following is an illustration of the dynamic model for the i^{th} generator, which can be found in the equations: [70].

$$\dot{\eth_t} = m_b(m_i - 1) \tag{19}$$

$$\dot{m_t} = \frac{1}{M}(P_{NI} - P_{ei} - P_{Di}) \tag{20}$$

$$\dot{e_q} = \frac{1}{T_{do}}[E_{fdi} - e_{qi} - (x_{di} - x_{di})i_{di}] \tag{21}$$

$$\dot{E_{fdl}} = \frac{1}{T_{Ei}}[K_{Ei}(v_{tri} - v_{ti} + u_{pssi}) - E_{fdi}] \tag{22}$$

All equation symbols have the same meaning. Approximations can linearize equations (19) to (22).

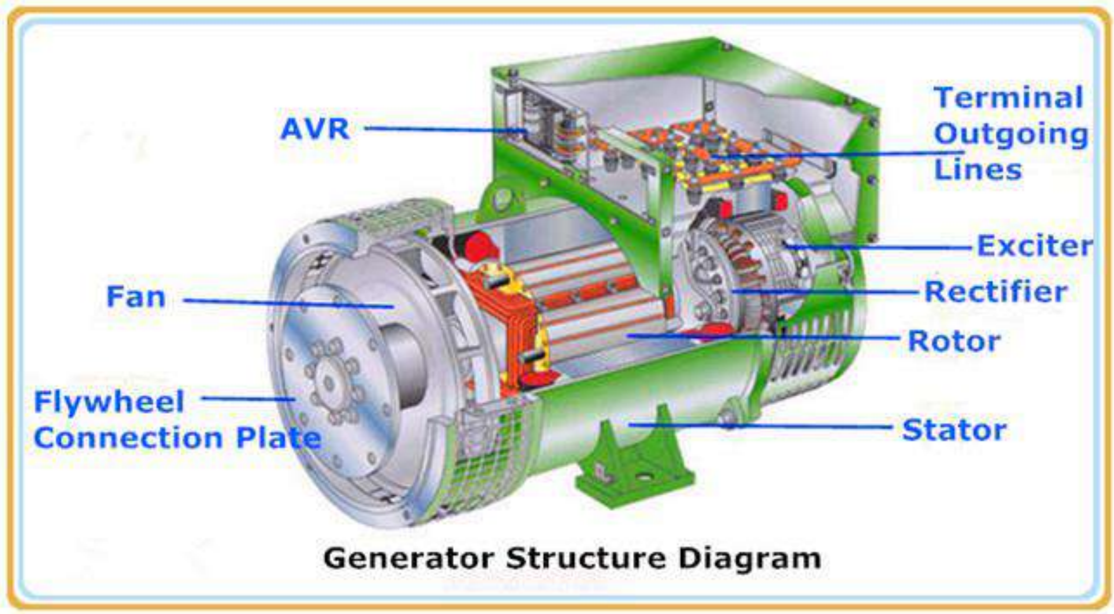

Fig. 4.3 Synchronous generator [71]

4.6 Bus Bar

A bus bar (also bus bar) is a metallic strip or bar used in electric power distribution, often in switchgear, panel boards, and busway enclosures. They connect high- and low-voltage battery electronics. Uninsulated and stiff, they're supported by insulated pillars. These features enable for appropriate conductor cooling and many tap-ins without a new junction.

4.7 Low Frequency Oscillation

Tiny signal stability addresses the ability of synchronous machines in an interconnected power system to sustain synchronism after a tiny disturbance. Depends on each synchronous machine's capacity to maintain electromagnetic and mechanical torque balance. After a disturbance, a synchronous machine's electromagnetic torque change may be divided into two components: a synchronizing torque component in phase with rotor angle deviation and a damping torque component in phase with speed deviation. A lack of synchronizing torque creates "aperiodic" or non-oscillatory instability, whereas a lack of dampening torque causes low-frequency oscillations. Generator rotor oscillations between 0.1 and 2.0 Hz are low frequency [13]. Electrical power oscillations are caused by an imbalance between demand and supply. Because early generators are intimately coupled to loads, power fluctuations are rare. Today's strong demand for electricity at the system's furthest end drives large power transfer across lengthy transmission lines, causing power oscillations. This is caused by rotor phase oscillation in a rotating frame. Increasing and lowering phase angle at a low frequency might affect power delivered from a synchronous machine. Local and inter-area LFOs exist [13][72].

- The swinging of units at a producing station in relation to the rest of the power system is known as local modes. Only a minor portion of the power grid experienced oscillations. The frequency range is typically 1-2 Hz.

- Many machines in one section of the system swing against machines in other areas of the system in interarea modes. Long tie lines are usually used in poorly linked power networks. The frequency range is typically 0.1-1 Hz.

Poor controller design can lead to additional modes [10]. Torsional oscillation occurs in series capacitor compensated systems and has a sub-synchronous frequency.

4.8 Experimental Details for Four Machine Two Area and IEEE-39 Bus Test System Using Tunicate Swarm Algorithm:

The TSA is assessed using models such as the IEEE-39 bus 10-machine system and the linearized 2-area four-machine network in multi-machine power system networks. These models are used in the evaluation of the TSA. Multi-machine power systems employ MATLAB-based simulations for **Fig. 4.4** and **Fig. 4.5**. There have been comparisons made between the outcomes of simulations for TSA-based PSS and PSO-based PSS, as well as comparisons between conventional and non-PSS. The issue dimensions are set to 5, 100, and 500 when employing the TSA and PSO procedures. The population size is represented by these numbers. The time constant for the reset block has been set to ten seconds (T_w). K_{ci} ideal parameter range was set to [0.0 to 50.0], whereas T_{1i} and T_{3i} optimal parameter ranges were set at [0.01 to 1.00].

For four machine A 3-φ fault was considered on bus 7 for 0.1 seconds which started at 0.5 seconds, and the simulation executed for 5 seconds in total.

For ten machine After every 0.5 seconds for 0.1 second, Bus 29 encounters a three phase balanced fault. The simulation is expected to endure for a total of 5 seconds. It's estimated that the simulation will take 5 seconds to complete.

4.8.1 Four Machine Two Area System

As illustrated in **Fig. 4.4**, the analyzed system (Kundur's four-machine two-area test system) comprises of two perfectly symmetrical regions connected by two 230 kV lines of 220 km length. Despite its modest size, it closely resembles the behavior of ordinary operating systems. Two identical 20kV/900MVA round rotor generators are installed in each location.

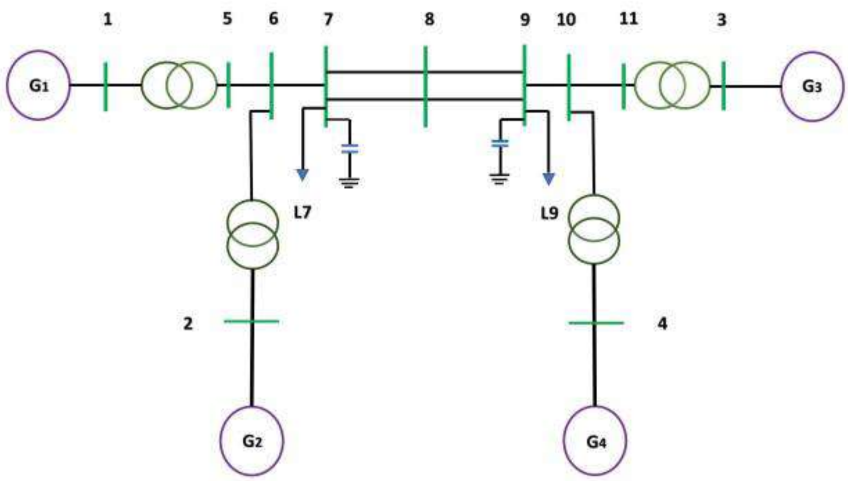

Fig. 4.4 Four-machine network in two area

4.8.2 IEE-39 Bus Test System Network

In this experimental system there have been no studies of the effect of the presence of a magnetic field on the dynamics of the system. this system have 10 generators 38 buses. Each region has two identical round rotor generators rated at 20kV/900MVA.

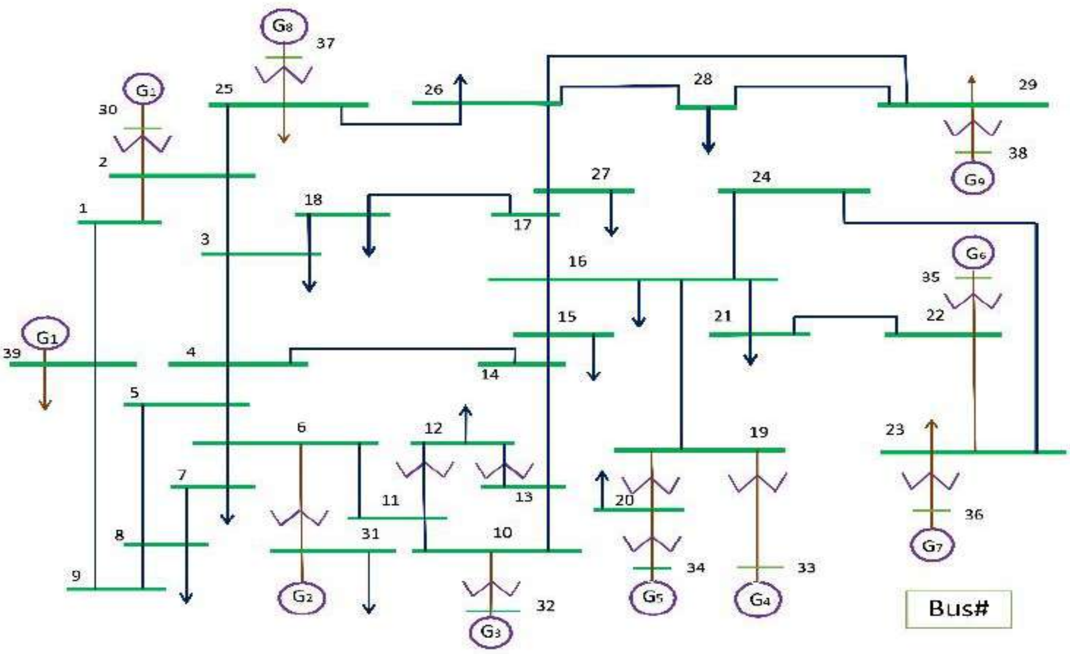

Fig. 4.5 IEEE 39-busses system test

4.9 Experimental Details for 4-Machine 2-Area and IEEE-39 Bus Test System Using Equilibrium Optimizer:

The efficiency of EO in multi-machine power system networks are examined using an IEEE-39 bus 10-machine system and a linearized two-area 4-machine model. EO efficacy in multi-machine power system networks is evaluated using a MATLAB simulation for **Fig. 4.6** and **Fig. 4.7** in this research. The greatest outcomes were found by contrasting PSS based on EO, PSS based on PSO, and standard PSS without PSS. The population size and total generation dimensions for EO techniques are 5, 100, and 500, respectively. Tw, the time constant for the reset block, has been set to 10 seconds by default. There were no ideal parameter ranges for T_{1i} or T_{3i}; instead, the ideal parameter ranges were [0.0 to 50.0].

For four machine Bus 7 has a 3-phase fault for 0.1 seconds commencing at 0.5 seconds, and the simulation will run a total of 5 seconds.

For ten machine Bus 29 suffers a three phase balanced fault after every 0.5 seconds for 0.1 second. Approximately 5 seconds are estimated to pass throughout the exercise.

4.9.1 *Four Machine Two Area System*

As seen in **Fig. 4.6**, the analyzed system is comprised of two 230 kV lines of 220 km length that connect two symmetrical pieces of land. Although it is compact, it closely resembles the behavior of real-world systems. Two 20kV/900MVA round rotor generators are installed in each location.

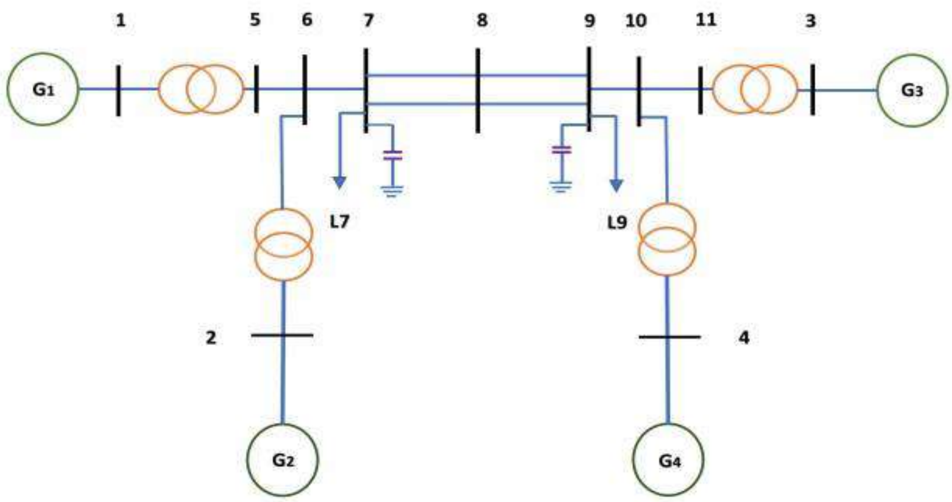

Fig. 4.6 Four-machine network in two area

4.9.2 IEEE-39 Bus Test System

Without a magnetic field, this experimental system has not been studied for its influence on its dynamics. There are 10 generators and 38 buses in this system shown in **Fig. 4.7**. There are two round rotor generators rated at 20kV/900MVA in each area of the country.

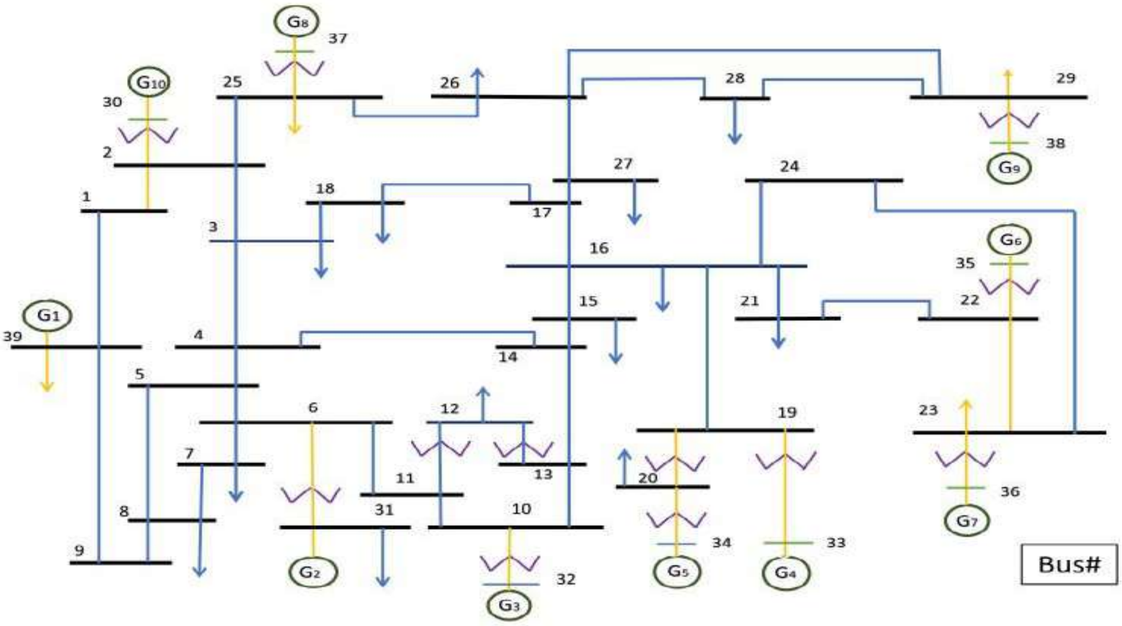

Fig. 4.7 A Test System for the IEEE 39-Bus

CHAPTER 5

RESULT AND DISCUSSIONS

5.1 Introduction

In this chapter, we discuss about the result by analysis the graph and data. we analyze the two optimization algorithms results by utilizing the optimal parameters. Each optimizer simulate by two example and they are two area four machine and IEEE 39 Bus. Four-machine network in two areas and a test system for IEEE 39-busses are shown by the figure very accurately. The value for the examples are shows in the tables. The examples are explain with many graphs like angular frequency shown against time, Time-relative Control Signal, G2's rotor angle in relation to time, Variation in the optimization goal function depending on TSA and EO which are give a clearly idea of our works.

5.2 Experimental results for tunicate swarm optimization:

In **Fig. 4.4**, a two-area, four-machine power system network is depicted and provides further information about the network data [13]. According to [13] , the TSA method was used to carry out the optimization process for three parameters, and the damping ratio for the system with that configuration can be found in [73].

5.2.1 Example 1: 4-Machine 2-Area Network

First of all when fault is applied to the system the whole system gets unstable. When fault is occurred the generators get excited. From the graph it is visible to us that the angular frequency (**Fig. 5.1**) of the four generators became stable with time. The fault applied at .5 second for a short time and the system get stable at 4 second. The system getting stable within 3.5 second.

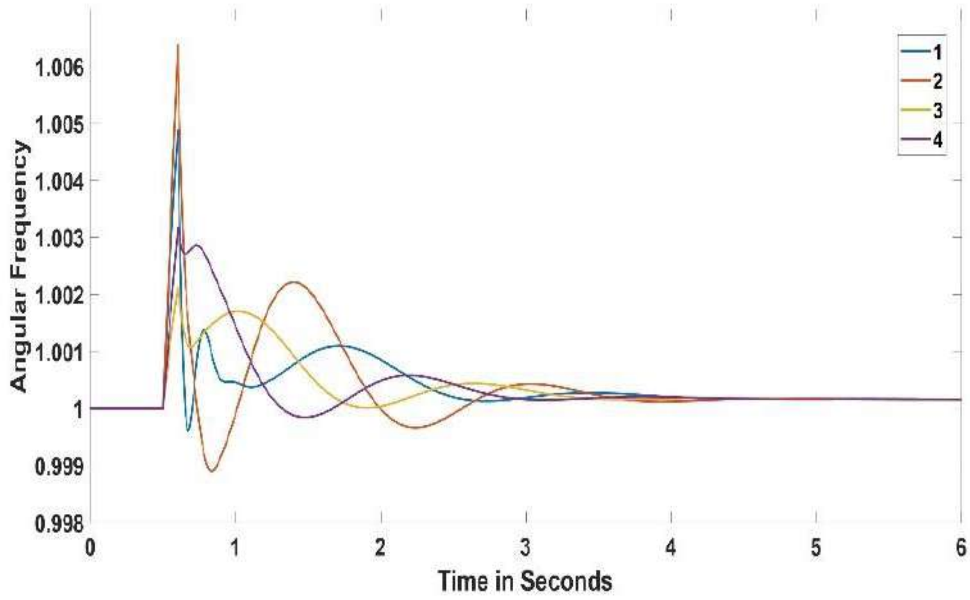

Fig. 5.1 4-generators angular frequency shown against time.

The **Fig. 5.2** below is shows us the control signal comparison between conventional PSS and TSA based PSS. In a system when a fault applied find a fine stabilization graph for TSA based PSS. And conventional PSS is take more time for getting stable. So we can justify the proposed algorithm is more efficient then conventional.

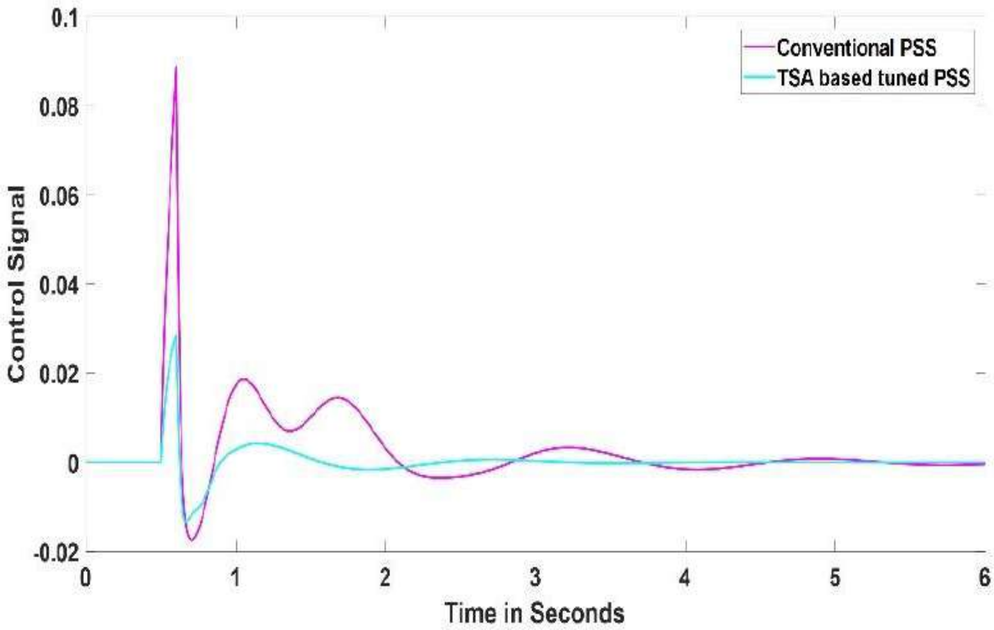

Fig. 5.2 Control Signal for G_2

One more comparison graph for justify proposed algorithm where it shows us the angular frequency (**Fig. 5.3**) with respect to time. For justifying we compare with a conventional PSS which angular frequency graph take time for getting stable. Beside the proposed algorithm graphs angular frequency is more better then conventional PSS.

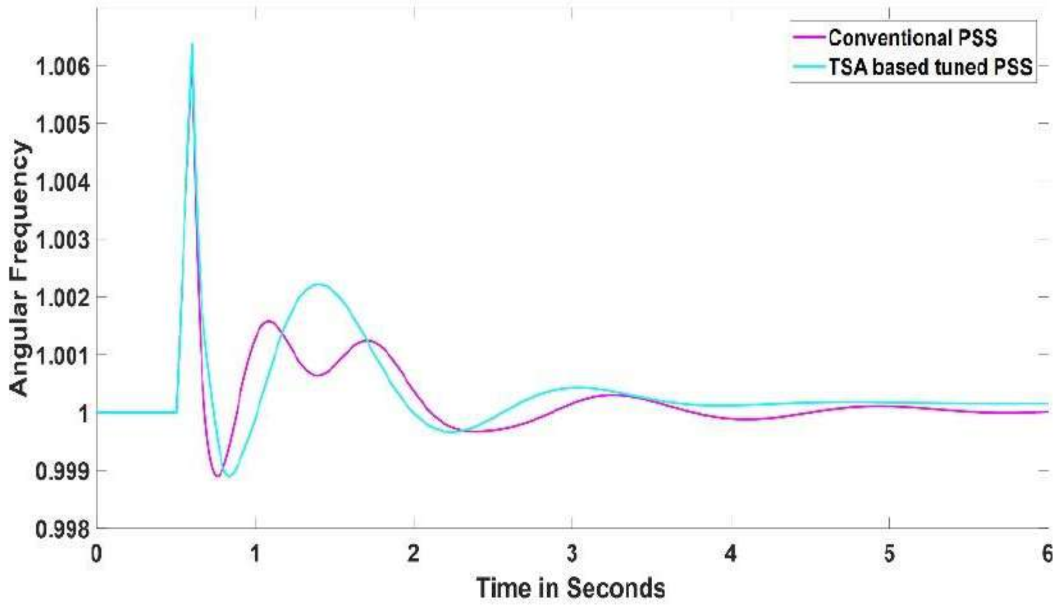

Fig. 5.3 Angular frequency for G_2

In this graph (**Fig. 5.4**) shows us the rotor angle comparison between TSA based PSS and conventional based PSS. In this figure shows the stabilization of rotor angle of generator 2 when a fault is applied to the system. TSA based PSS is more better than conventional PSS.

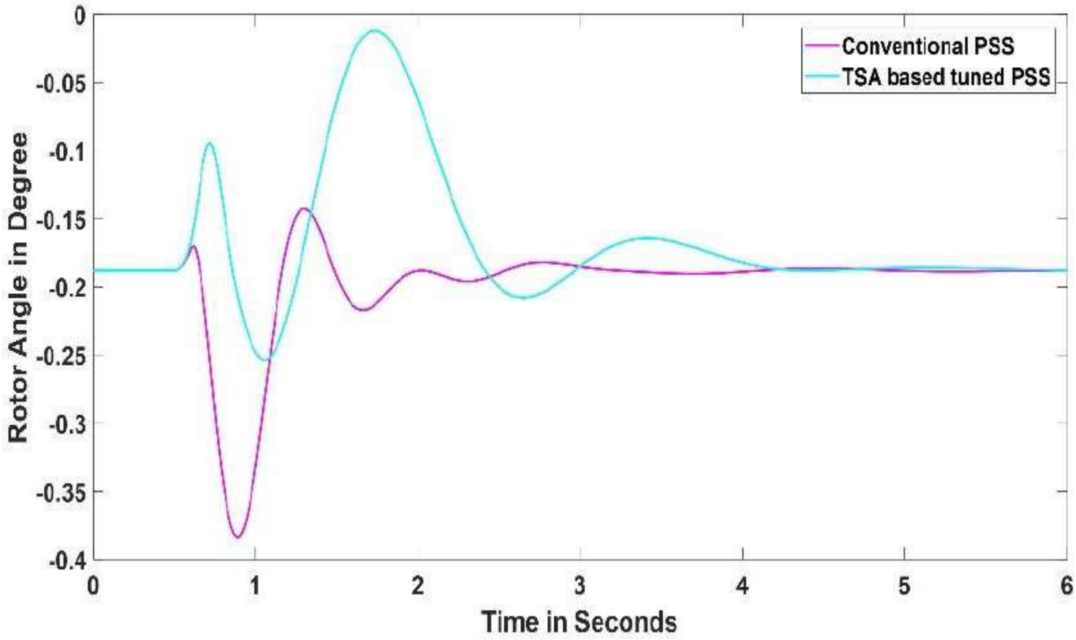

Fig. 5.4 Rotor angle for G_2

In this graph shows the variations of objection function (**Fig. 5.5**). For the MATLAB simulation we have a objection function and iteration number is 500.

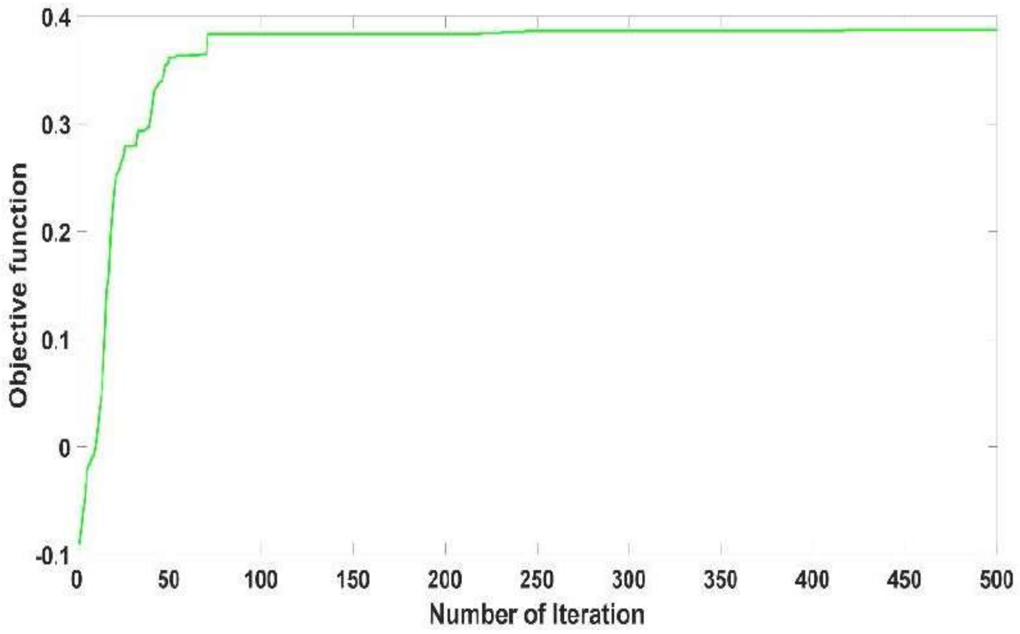

Fig. 5.5 Variation in the optimization goal function depending on TSA.

Table 5.1 illustrates the ideal values of various parameters such as Kc, T_1, and T_3 for the four machine network's distinct generators, while **Table 5.2** shows the lowest damping ratio for various PSS types such as classic PSS, PSO-based PSS, and TSA-based PSS. In terms of minimal damping ratio, the suggested TSA-based PSS performs 2.6 times better than traditional PSS and 1.3 times better than PSO-based PSS, according to the comparison analysis.

Table 5.1 4-machine TSA network settings

Gen. No	Parameters		
	K_c	T_1	T_3
G_1	19.95860	0.04404	0.44983
G_2	3.54701	0.01481	0.11798
G_3	50	0.24148	0.05201
G4	0.05182	0.32099	0.29672

Table 5.2 PSS Minimum Damping Ratio Measurement.

Conventional PSS	PSO optimized PSS	TSA optimized PSS
0.1558	0.3220	0.4091

5.2.2 Example 2: Testing System for IEEE-39 Bus Standards

The IEEE-39 bus will be demonstrated using a ten-machine power system network in Fig. 9 from New England. There is a lot of information in [74] about the system. PSS parameters for a specific base instance will be altered using a TSA-based technique [74].

In this figure, rotor angle variations with time has been showed for TSA. As it shown (**Fig. 5.6**), TSA has been stabled after some time when conventional is not. We can say that algorithm worked very well for rotor angle in TSA.

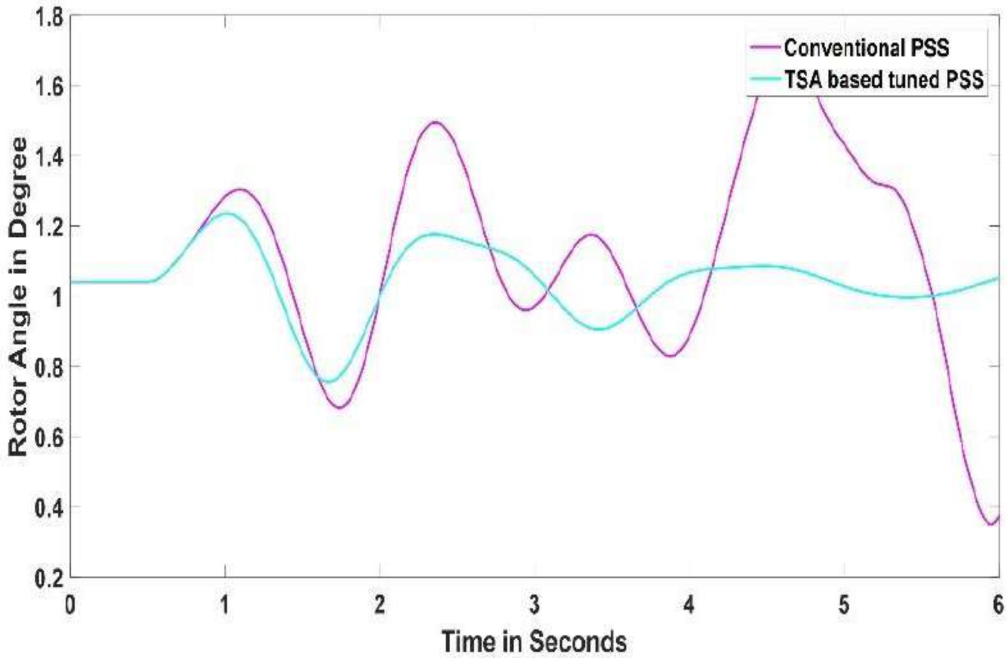

Fig. 5.6 Rotor angle for G_3

Secondly In the figure, control signal variations with time has been showed for TSA. As it shown in **Fig. 5.7**, Conventional has not been stabled with time. We can say that algorithm worked very well for rotor angle in TSA.

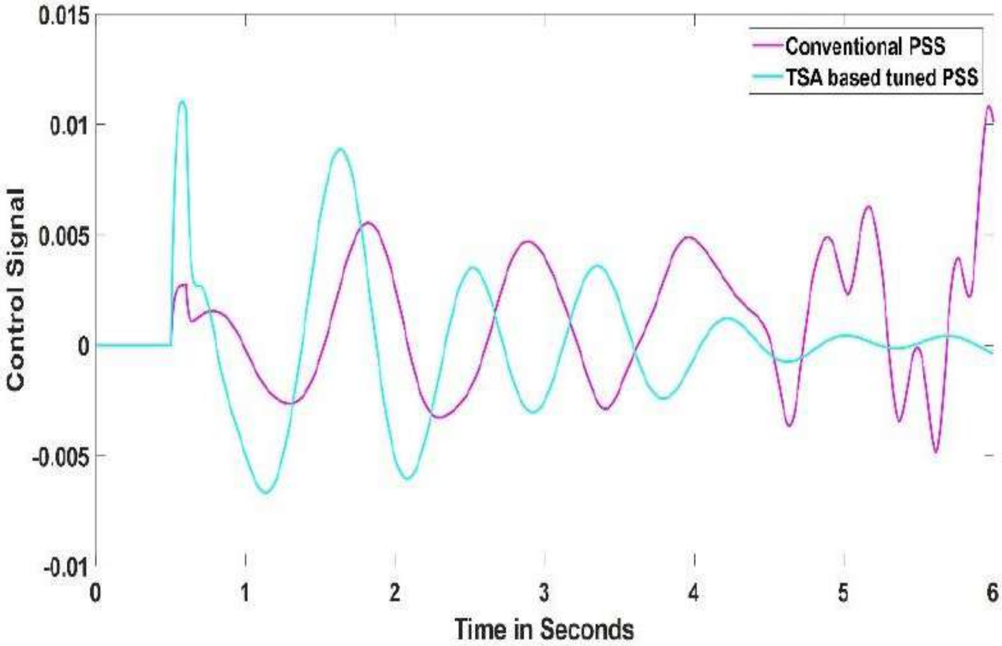

Fig. 5.7 Control Signal for the G_3

The angular frequency with respect to time is depicted in yet another comparison graph (**Fig. 5.8**) to support the suggested technique. Using a standard PSS whose angular frequency graph takes time to become stable as an example, we can see that our argument is sound. The suggested technique, as well as the graphs of angular frequency, outperforms the usual PSS algorithm.

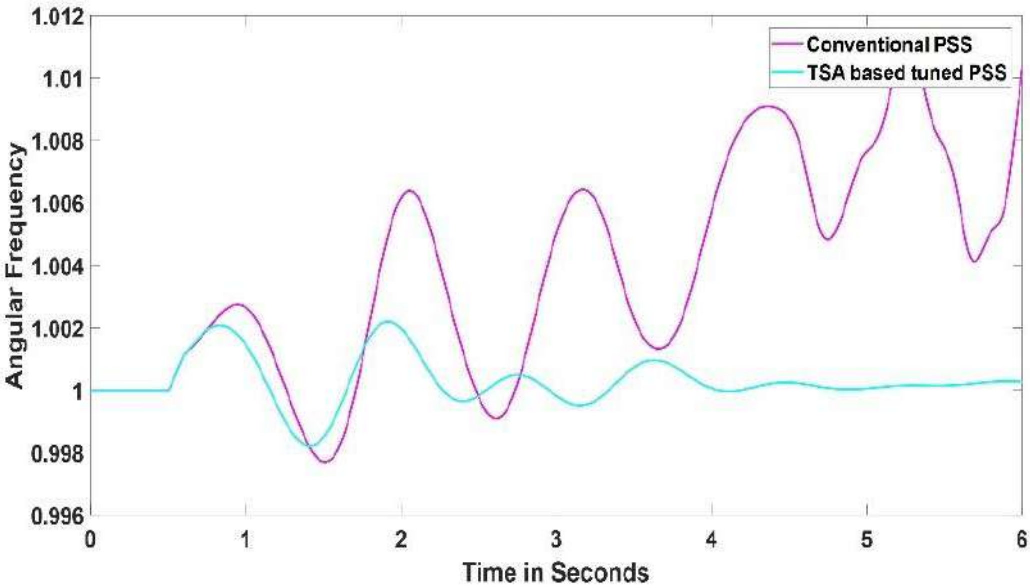

Fig. 5.8 Angular frequency for G_3

In a ten-machine power system network, **Table-5.3** illustrates the minimum damping ratio for TSA-optimized, PSO-optimized, and traditional PSS. TSA-based PSS delivers 5 times greater damping ratio than traditional PSS and 6.5 times better than PSO-based PSS**. Table 5.4** displays TSA-optimized parameter values.

Table 5.3 Minimum Damping Ratio of different PSS Types

Without PSS	**PSO optimized PSS**	**TSA optimized PSS**
-0.0334	0.0264	0.1720

Table 5.4 Parameters for TSA-Optimized of 10-Machine Network

Gen. No	**Parameters**		
	K_c	**T_1**	**T_3**
G_1	0	0	0
G_2	38.041438	0.783165	0.427126
G_3	20.021337	0.587660	0.541127
G_4	34.319470	0.715801	1
G_5	5.636783	0.4618734	0.405703
G_6	7.490372	0.968557	0.827961
G_7	9.319073	0.060181	0.716414
G_8	28.237234	0.955893	0.886527
G_9	37.693815	0.114877	0.328012
G_{10}	50	0.833852	0.826006

5.3 Experimental results for Equilibrium Optimizer

5.3.1 Example 1: 4-machine network in 2-areas

Detailed information about the network data is provided in [13] for the two-area, four-machine power system network illustrated in Fig. 3. The optimization method was carried out for three parameters using the EO approach for a given base case [13], furthermore in [73], the damping ratio for the system with the same design is provided.

In the first place, when a flaw is introduced into a system, the entire system becomes unstable. Generators become overexcited when a problem has occurred. The graph **Fig. 5.9** shows that the angular frequency of the four generators got more stable with time, as can be seen in the graph. It took only .5 seconds for the fault to be applied and the system to become stable at 4 seconds. Within 3.5 seconds, the system becomes steady.

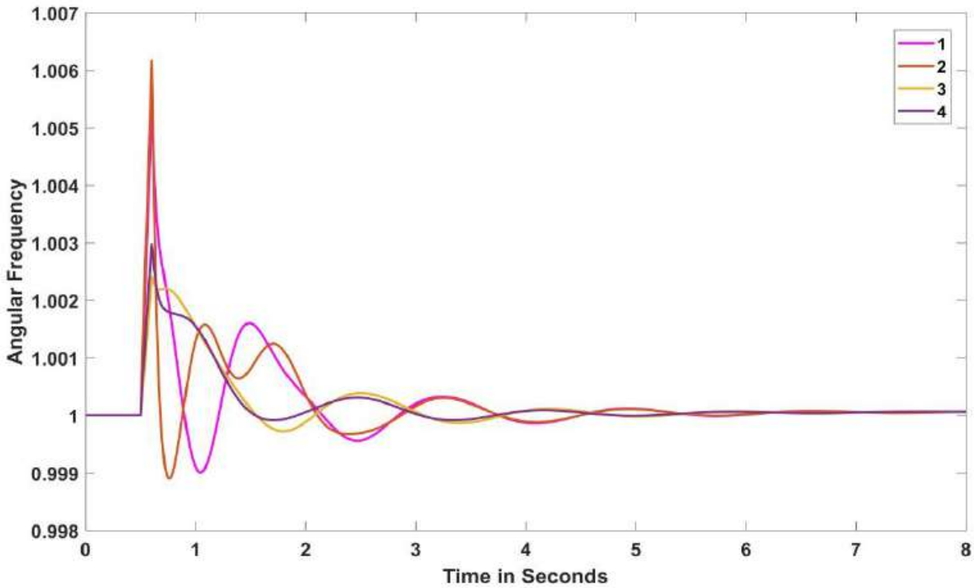

Fig. 5.9 Four-generators angular frequency with relation to time

The control signal comparison between traditional PSS and EO-based PSS is depicted in the picture **Fig. 5.10**. When a failure is applied to a system, discover a fine stabilization graph for EO-based PSS that is suitable. Furthermore, traditional PSS requires more time to get stabilized. As a result, we can demonstrate that the suggested approach is more efficient than the standard technique.

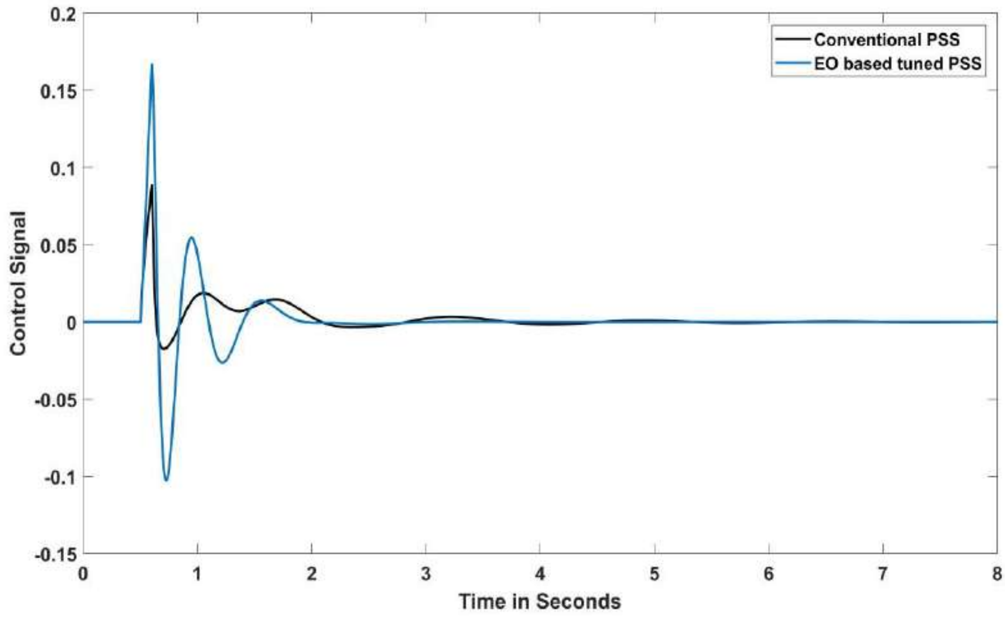

Fig. 5.10 Control Signal for G_2

One additional comparison graph to support the suggested technique, this one displaying the angular frequency with respect to time, is shown in **Fig. 5.11**. For the purpose of justification, we will compare this to a traditional PSS, whose angular frequency graph takes time to become stable. Aside from the suggested technique, graphs with angular frequency are superior to those obtained with standard PSS.

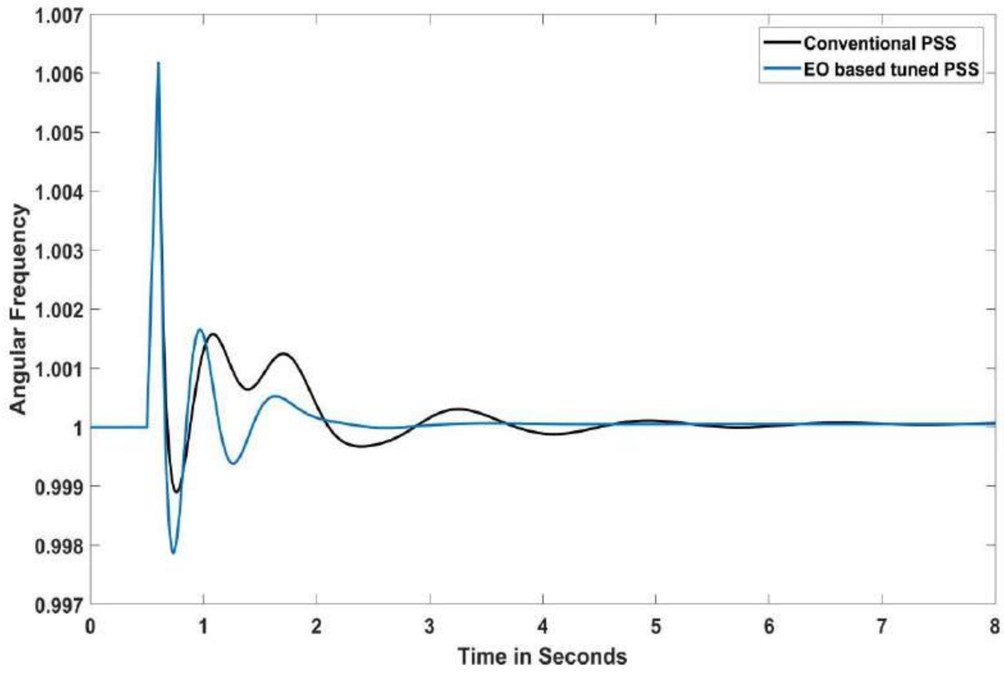

Fig. 5.11 Angular frequency for G_2

Using this graph **Fig. 5.12**, we can see a comparison between EO-based PSS and conventional-based PSS in terms of rotor angle. When a defect is introduced to the system, the stabilization of the rotor angle of generator 2 is depicted in this illustration. EO-based PSS outperforms traditional PSS in terms of effectiveness.

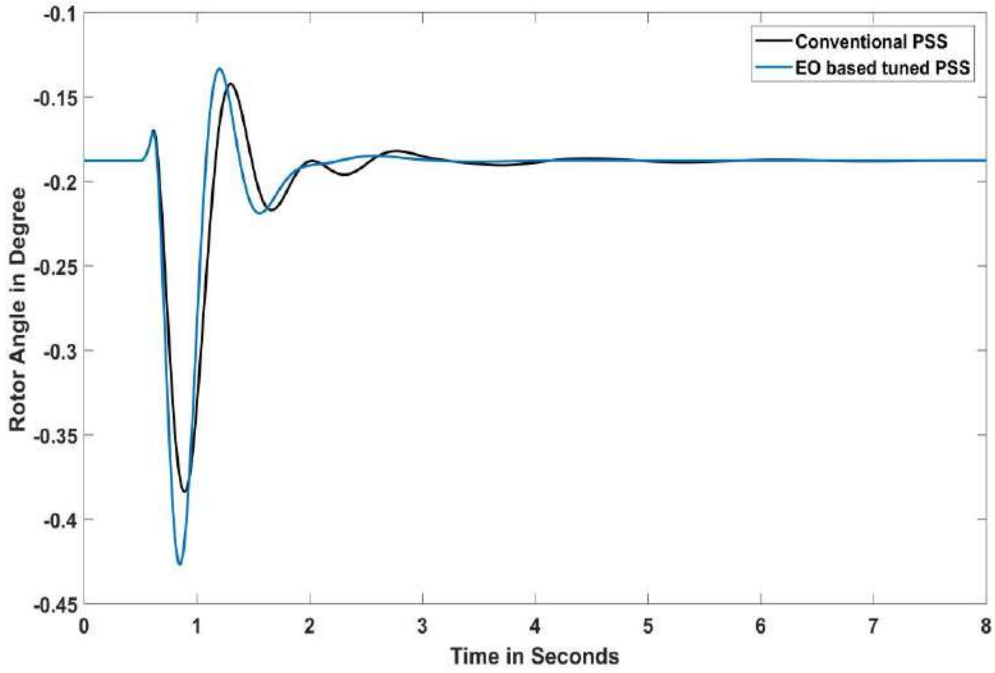

Fig. 5.12 Rotor angle for G_2

The fluctuations of the objection function are seen in this graph **Fig. 5.13**. Iteration number 500 is used for the MATLAB simulation, and an objection function is used in the simulation.

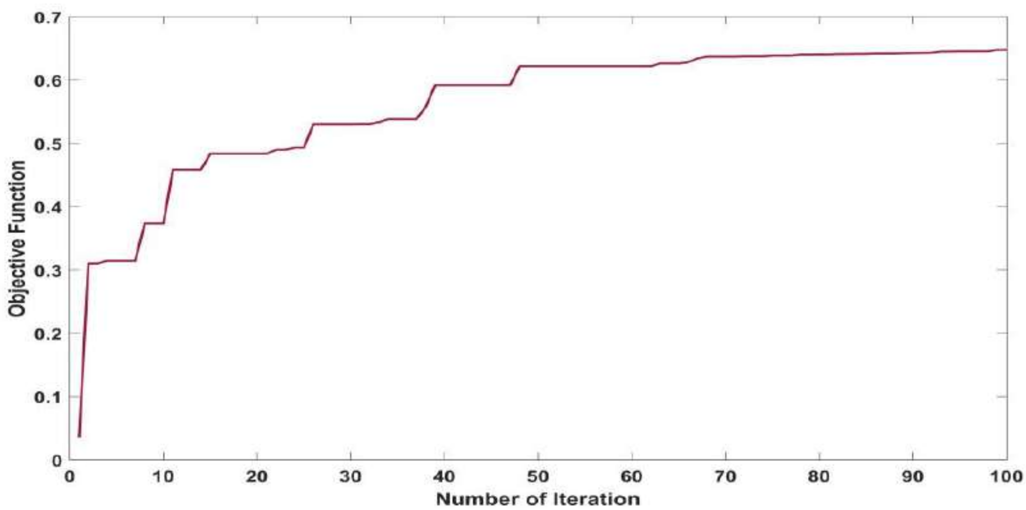

Fig. 5.13 Variation of the goal function in the context of the EO-based optimization approach.

Table 5.5 illustrates appropriate Kc, T1, and T3 values for four-machine network generators. **Table 5.6** shows the damping ratio for classical, PSO-based, and EO-based PSS. The suggested EO-based PSS provides 4.15 times greater damping ratio than traditional PSS and 2 times better than PSO-based PSS.

Table 5.5 Parameters Optimized for Four-Machine Network Utilizing EO

Gen. No	**Parameters**		
	K_c	**T_1**	**T_3**
G_1	19.95860	0.04404	0.44983
G_2	3.54701	0.01481	0.11798
G_3	50	0.24148	0.05201
G_4	0.05182	0.32099	0.29672

Table 5.6 In order to get the lowest damping ratio, various PSS types tested.

Conventional PSS	**PSO optimized PSS**	**EO optimized PSS**
0.1558	0.3220	0.6477

5.3.2 Example 2: Testing System for IEEE-39 BUS Standards

The IEEE-39 bus will be demonstrated in this example using a 10-machine power system network of New England's IEEE-39 bus, as seen in Fig. 9. In-depth details about the system may be found in [74]. A EO-based technique has been used in order to modify the PSS parameters for a specific base instance [74].

Rotor angle variations with time have been shown in this **Fig. 5.14** for the time-domain analysis (EO). As demonstrated, EO has stabilized over a period of time, but conventional has not. In terms of rotor angle in EO, we can claim that the algorithm performed admirably.

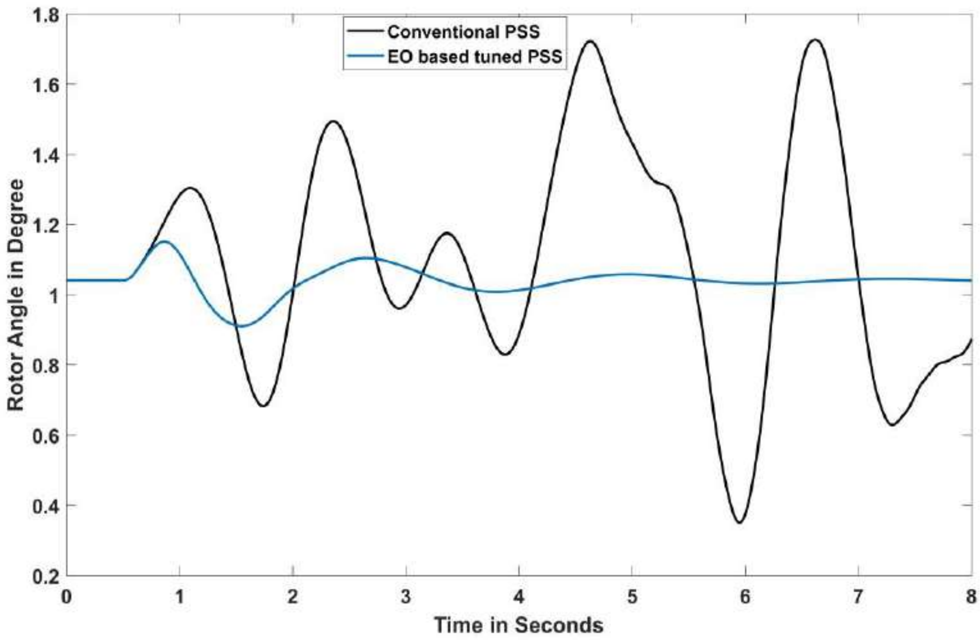

Fig. 5.14 Rotor angle for G_3

Secondly EO's control signal fluctuations with time have been depicted in the **Fig. 5.15** to the right. As has been seen, conventional has not been steady throughout time. In terms of rotor angle in EO, we can claim that the algorithm performed admirably.

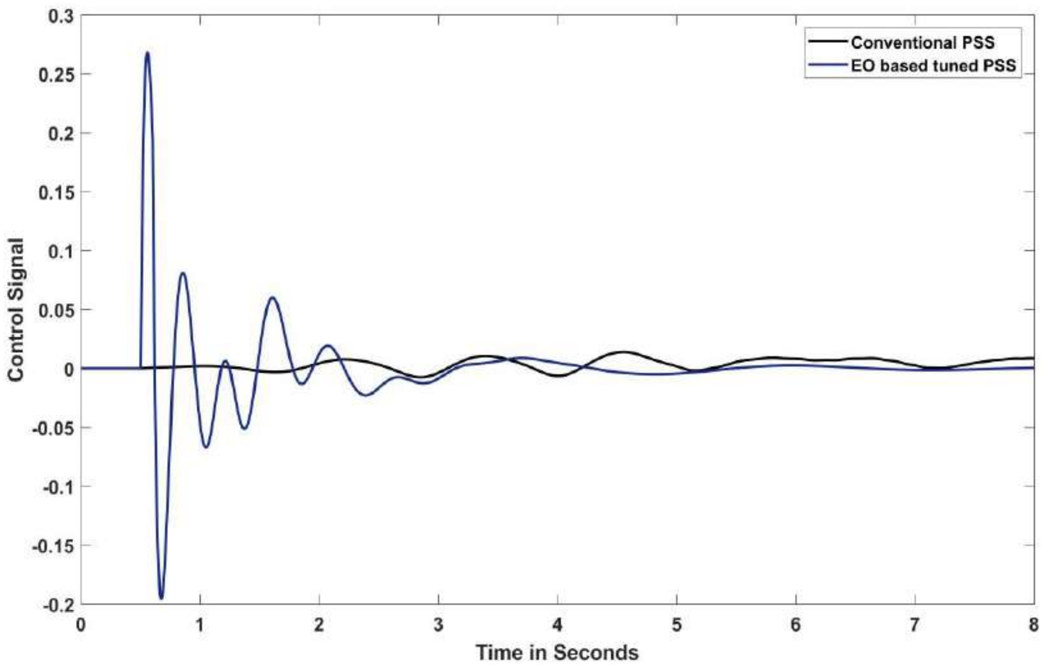

Fig. 5.15 Control Signal for G_3

The angular frequency with respect to time is depicted in yet another comparison graph **Fig. 5.16** to support the suggested technique. Using a standard PSS whose angular frequency graph takes time to become stable as an example, we can see that our argument is sound. The suggested technique, as well as the graphs of angular frequency, outperforms the usual PSS algorithm.

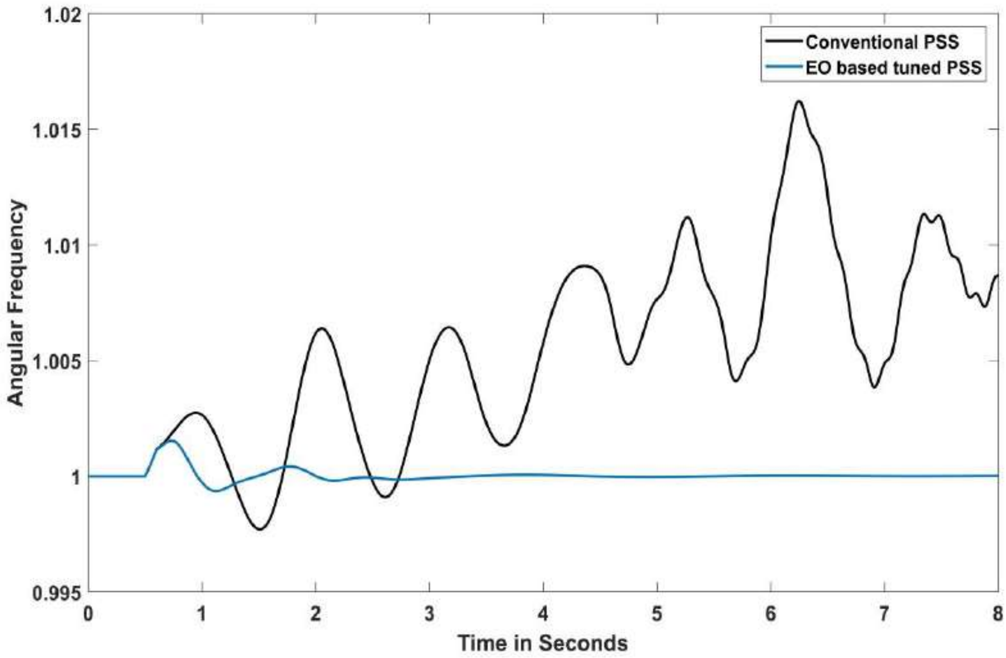

Fig. 5.16 Angular frequency for G_3

In **Table-5.7** showing the minimal damping ratio derived using eigenvalue analysis for a system and configuration that are identical. According to eigenvalue analysis, the least damping ratio achieved is larger than the least damping ratio obtained by doing PSO analysis. A type of eigenvalue analysis is the eigenvalue analysis. From comparative results, it can be seen that the TSA-based PSS gives 5.4 times better result than conventional PSS and 7 times better result than PSO-based PSS in terms of damping ratio. **Table-5.8** provides an overview of the EO-based optimized parameters as well as their associated values for each parameter.

Table 5.7 Different PSS Types Tested to Get the Lowest Damping Ratio

Without PSS	PSO optimized PSS	EO optimized PSS
-0.0334	0.0264	0.1720

Table 5.8 EO-Based Optimization of Four-Machine Network Parameters

Gen. No	Parameters		
	K_c	T_1	T_3
G_1	0	0	0
G_2	38.041438	0.783165	0.427126
G_3	20.021337	0.587660	0.541127
G_4	34.319470	0.715801	1
G_5	5.636783	0.4618734	0.405703
G_6	7.490372	0.968557	0.827961
G_7	9.319073	0.060181	0.716414
G_8	28.237234	0.955893	0.886527
G_9	37.693815	0.114877	0.328012
G_{10}	50	0.833852	0.826006

CHAPTER 6

CONCLUSION

6.1 Introduction

In this chapter, we give an over view about the whole work. Future scope and limitations are also mentioned.

6.2 Conclusion

The Equilibrium Optimizer (EO) and the tunicate swarm algorithm (TSA) approach are both useful methods that utilized in the design of power system stabilizers for multi-machine power systems. The results of this study indicate that the probabilistic EO and TSA perform significantly better than the CPSS and PSO in practically every aspect of the tests that are carried out. Multi-objective optimization proved to be the most successful method of dealing with this problem conclusion. The performance and resiliency of an EO-based PSS and a TSA-based PSS are analyzed using four machines 11 buses and a multi-system network of ten machines 39 buses. The findings indicate that the recently developed heuristic technique provides superior performance, and the capability of the method to arrive at convergence regardless of the starting guess demonstrates the robustness of the method. In the end, the outcomes of the EO-optimized PSS and TSA-optimized PSS are compared with the well-established PSO-optimized PSS and the conventional PSS. According to the findings of a comparative research, the EO-based PSS and TSA-based PSS methods produce superior results in terms of damping ratio compared to the PSO-based approach and the traditional method. This algorithm can be used to design robust PSS models for multi-machine power systems using EO and TSA.

REFERENCES

[1] M. Shafiullah, M. A. Abido, and L. S. Coelho, "Design of robust PSS in multimachine power systems using backtracking search algorithm," *2015 18th Int. Conf. Intell. Syst. Appl. to Power Syst. ISAP 2015*, 2015, doi: 10.1109/ISAP.2015.7325528.

[2] A. Ghasemi, H. Shayeghi, and H. Alkhatib, "Robust design of multimachine power system stabilizers using fuzzy gravitational search algorithm," *Int. J. Electr. Power Energy Syst.*, vol. 51, pp. 190–200, 2013, doi: 10.1016/j.ijepes.2013.02.022.

[3] H. Shayeghi, S. Jalilzadeh, H. A. Shayanfar, and A. Safari, "Robust PSS design using chaotic optimization algorithm for a multimachine power system," *2009 6th Int. Conf. Electr. Eng. Comput. Telecommun. Inf. Technol. ECTI-CON 2009*, vol. 1, pp. 40–43, 2009, doi: 10.1109/ECTICON.2009.5136961.

[4] Z. Jiang, "Design of a nonlinear power system stabilizer using synergetic control theory," *Electr. Power Syst. Res.*, vol. 79, no. 6, pp. 855–862, 2009, doi: 10.1016/j.epsr.2008.11.006.

[5] M. J. Gibbard, "ROBUST DESIGN OF FIXED-PARAMETER POWER SYSTEM STABILISERS OVER A WIDE RANGE OF OPERATING CONDITIONS," vol. 6, no. 2, 1991.

[6] G. Naresh, M. Ramalinga Raju, and M. Sai Krishna, "Design and parameters optimization of multi-machine power system stabilizers using artificial bee colony algorithm," *2012 Int. Conf. Adv. Power Convers. Energy Technol. APCET 2012*, 2012, doi: 10.1109/APCET.2012.6302066.

[7] Z. Wang, C. Y. Chung, K. P. Wong, and C. T. Tse, "Robust power system stabiliser design under multi-operating conditions using differential evolution," *IET Gener. Transm. Distrib.*, vol. 2, no. 5, pp. 690–700, 2008, doi: 10.1049/iet-gtd:20070449.

[8] A. Farah, T. Guesmi, H. Hadj Abdallah, and A. Ouali, "Optimal design of multimachine power system stabilizers using evolutionary algorithms," *2012 1st Int. Conf. Renew. Energies Veh. Technol. REVET 2012*, pp. 497–502, 2012, doi: 10.1109/REVET.2012.6195319.

[9] M. A. Abido, "Robust design of multimachine power system stabilizers using simulated annealing," *IEEE Trans. Energy Convers.*, vol. 15, no. 3, pp. 297–304, 2000, doi: 10.1109/60.875496.

[10] E. S. Ali and S. M. Abd-Elazim, "Optimal power system stabilizers design for multimachine power system via hybrid approach," *J. Electr. Eng.*, vol. 13, no. 3, pp. 83–90, 2013.

[11] S. Kaur, L. K. Awasthi, A. L. Sangal, and G. Dhiman, "Tunicate Swarm Algorithm: A new bio-inspired based metaheuristic paradigm for global optimization," *Eng. Appl. Artif. Intell.*, vol. 90, no. November 2019, p. 103541, 2020, doi: 10.1016/j.engappai.2020.103541.

[12] A. Faramarzi, M. Heidarinejad, B. Stephens, and S. Mirjalili, "Equilibrium optimizer: A novel optimization algorithm," *Knowledge-Based Syst.*, vol. 191, 2020, doi: 10.1016/j.knosys.2019.105190.

[13] P. Kundur, "Power System Stability And Control by Prabha Kundur.pdf," *McGraw-Hill, Inc*. p. 1167, 1994.

[14] K. Chakraborty and A. Chakrabarti, *Modern Power System Analysis*, 4th editio. 2015.

[15] L. Summary-, D. Equation, S. M. Power, S. Stability, and D. Stability, "Power System Stability Lesson Summary-1:-1. Introduction 2. Classification of Power System Stability 3. Dynamic Equation of Synchronous Machine."

[16] S. Y. Caliskan and P. Tabuada, "Compositional transient stability analysis of multimachine power networks," *IEEE Trans. Control Netw. Syst.*, vol. 1, no. 1, pp. 4–14, 2014, doi: 10.1109/TCNS.2014.2304868.

[17] A. T. Submitted, I. N. Partial, F. Of, R. For, and T. H. E. Degree, "Design of Power System Design of Power System," no. May, 2012.

[18] A. E. Leon, J. M. Mauricio, and J. A. Solsona, "Multi-machine power system stability improvement using

an observer-based nonlinear controller," *Electr. Power Syst. Res.*, vol. 89, pp. 204–214, Aug. 2012, doi: 10.1016/J.EPSR.2012.01.022.

[19] R. Devarapalli, B. Bhattacharyya, N. K. Sinha, and B. Dey, "Amended GWO approach based multi-machine power system stability enhancement," *ISA Trans.*, vol. 109, pp. 152–174, 2021, doi: 10.1016/j.isatra.2020.09.016.

[20] H. Shayeghi, A. Safari, and H. A. Shayanfar, "PSS and TCSC damping controller coordinated design using PSO in multi-machine power system," *Energy Convers. Manag.*, vol. 51, no. 12, pp. 2930–2937, 2010, doi: 10.1016/j.enconman.2010.06.034.

[21] G. Shahgholian, A. Movahedi, and J. Faiz, "Coordinated Design of TCSC and PSS Controllers using VURPSO and Genetic Algorithms for Multi-Machine Power System Stability," vol. 13, pp. 1–12, 2015, doi: 10.1007/s12555-013-0387-z.

[22] A. B. Khormizi and A. S. Nia, "Damping of power system oscillations in multi-machine power systems using coordinate design of PSS and TCSC," *2011 10th Int. Conf. Environ. Electr. Eng. EEEIC.EU 2011 - Conf. Proc.*, vol. 1, no. 1, pp. 11–14, 2011, doi: 10.1109/EEEIC.2011.5874795.

[23] E. Nechadi, M. N. Harmas, A. Hamzaoui, and N. Essounbouli, "A new robust adaptive fuzzy sliding mode power system stabilizer," *Int. J. Electr. POWER ENERGY Syst.*, vol. 42, no. 1, pp. 1–7, 2012, doi: 10.1016/j.ijepes.2012.03.032.

[24] H. Huerta, A. G. Loukianov, and J. M. Cañedo, "Multimachine Power-System Control : Integral-SM Approach," vol. 56, no. 6, pp. 2229–2236, 2009.

[25] H. E. Psillakis and A. T. Alexandridis, "A new excitation control for multimachine power systems II: Robustness and disturbance attenuation analysis," *Int. J. Control. Autom. Syst.*, vol. 3, no. 2 SPEC. ISS., pp. 288–295, 2005.

[26] R. Mahanty and P. Gupta, "Voltage stability analysis in unbalanced power systems by optimal power flow," *IEE Proceedings-Generation, Transm. …*, vol. 151, no. 3, pp. 201–212, 2004, doi: 10.1049/ip-gtd.

[27] T. Guesmi, A. Farah, H. H. Abdallah, and A. Ouali, "Robust design of multimachine power system stabilizers based on improved non-dominated sorting genetic algorithms," *Electr. Eng.*, vol. 100, no. 3, pp. 1351–1363, 2018, doi: 10.1007/s00202-017-0589-0.

[28] M. A. Mahmud, M. J. Hossain, H. R. Pota, and A. M. T. Oo, "Robust Partial Feedback Linearizing Excitation Controller Design for Multimachine Power Systems," *IEEE Trans. Power Syst.*, vol. 32, no. 1, pp. 3–16, 2017, doi: 10.1109/TPWRS.2016.2555379.

[29] Z. Bouchama, N. Essounbouli, M. N. Harmas, A. Hamzaoui, and K. Saoudi, "Reaching phase free adaptive fuzzy synergetic power system stabilizer," *Int. J. Electr. Power Energy Syst.*, vol. 77, pp. 43–49, 2016, doi: 10.1016/j.ijepes.2015.11.017.

[30] V. Pant, B. Das, and A. Bhargava, "Periodic output feedback technique based design of STATCOM damping controller," *Int. J. Electr. Power Energy Syst.*, vol. 43, no. 1, pp. 344–350, 2012, doi: 10.1016/j.ijepes.2012.05.005.

[31] R. Hemmati, M. Nikzad, and S. S. S. Farahani, "Investigation of UPFC performance under system uncertainties," *Int. J. Electr. Power Energy Syst.*, vol. 43, no. 1, pp. 1137–1143, 2012, doi: 10.1016/j.ijepes.2012.05.031.

[32] S. Shojaeian, J. Soltani, and G. Arab Markadeh, "Damping of low frequency oscillations of multi-machine multi-UPFC power systems, based on adaptive input-output feedback linearization control," *IEEE Trans. Power Syst.*, vol. 27, no. 4, pp. 1831–1840, 2012, doi: 10.1109/TPWRS.2012.2194313.

[33] K. Saoudi and M. N. Harmas, "Enhanced design of an indirect adaptive fuzzy sliding mode power system stabilizer for multi-machine power systems," *Int. J. Electr. Power Energy Syst.*, vol. 54, pp. 425–431, 2014, doi: 10.1016/j.ijepes.2013.07.034.

[34] R. K. Patnaik and P. K. Dash, "Fast adaptive back-stepping terminal sliding mode power control for both

the rotor-side as well as grid-side converter of the doubly fed induction generator-based wind farms," *IET Renew. Power Gener.*, vol. 10, no. 5, pp. 598–610, 2016, doi: 10.1049/iet-rpg.2015.0286.

[35] J. Deng, C. Li, and X. P. Zhang, "Coordinated Design of Multiple Robust FACTS Damping Controllers: A BMI-Based Sequential Approach with Multi-Model Systems," *IEEE Trans. Power Syst.*, vol. 30, no. 6, pp. 3150–3159, 2015, doi: 10.1109/TPWRS.2015.2392153.

[36] X. G. Yan, C. Edwards, S. K. Spurgeon, and J. A. M. Bleijs, "Decentralised sliding-mode control for multimachine power systems using only output information," *IEE Proc. Control Theory Appl.*, vol. 151, no. 5, pp. 627–635, 2004, doi: 10.1049/ip-cta:20040956.

[37] T. K. Roy, M. A. Mahmud, W. Shen, and A. M. T. Oo, "Non-linear adaptive coordinated controller design for multimachine power systems to improve transient stability," *IET Gener. Transm. Distrib.*, vol. 10, no. 13, pp. 3353–3363, 2016, doi: 10.1049/iet-gtd.2016.0377.

[38] M. A. Mahmud, H. R. Pota, M. Aldeen, and M. J. Hossain, "Partial feedback linearizing excitation controller for multimachine power systems to improve transient stability," *IEEE Trans. Power Syst.*, vol. 29, no. 2, pp. 561–571, 2014, doi: 10.1109/TPWRS.2013.2283867.

[39] T. Fetouh and M. S. Zaky, "New approach to design SVC-based stabiliser using genetic algorithm and rough set theory," *IET Gener. Transm. Distrib.*, vol. 11, no. 2, pp. 372–382, 2017, doi: 10.1049/iet-gtd.2016.0701.

[40] H. Kang, Y. Liu, Q. H. Wu, and X. Zhou, "Switching Excitation Controller for Enhancement of Transient Stability of Multi-machine Power Systems," vol. 1, no. 3, pp. 86–93, 2015.

[41] M. Farahani, "A Multi-Objective Power System Stabilizer," pp. 1–8, 2012.

[42] P. He, F. Wen, G. Ledwich, Y. Xue, and K. Wang, "Effects of various power system stabilizers on improving power system dynamic performance," *Int. J. Electr. Power Energy Syst.*, vol. 46, no. 1, pp. 175–183, 2013, doi: 10.1016/j.ijepes.2012.10.026.

[43] F. M. Hughes, "Power System Stabilizers Design for Interconnected Power Systems Gurunath," *Electron. Power*, vol. 23, no. 9, p. 739, 1977, doi: 10.1049/ep.1977.0418.

[44] H. Hasanvand, M. R. Arvan, B. Mozafari, and T. Amraee, "Coordinated design of PSS and TCSC to mitigate interarea oscillations," *Int. J. Electr. POWER ENERGY Syst.*, vol. 78, pp. 194–206, 2016, doi: 10.1016/j.ijepes.2015.11.097.

[45] S. Hameed, B. Das, and V. Pant, "Reduced rule base self-tuning fuzzy PI controller for TCSC," *Int. J. Electr. Power Energy Syst.*, vol. 32, no. 9, pp. 1005–1013, 2010, doi: 10.1016/j.ijepes.2010.02.004.

[46] J. Zhang, J. Y. Wen, S. J. Cheng, S. Member, and J. Ma, "A Novel SVC Allocation Method for Power System Voltage Stability Enhancement by Normal Forms of Diffeomorphism," vol. 22, no. 4, pp. 1819–1825, 2007.

[47] H. Zhao, X. Lan, N. Xue, and B. Wang, "Excitation prediction control of multi-machine power systems using balanced reduced model," *IET Gener. Transm. Distrib.*, vol. 8, no. 6, pp. 1075–1081, 2014, doi: 10.1049/iet-gtd.2013.0609.

[48] H. Liu, X. Xie, L. Wang, and Y. Han, "Optimal design of linear subsynchronous damping controllers for stabilising torsional interactions under all possible operating conditions," *IET Gener. Transm. Distrib.*, vol. 9, no. 13, pp. 1652–1661, 2015, doi: 10.1049/iet-gtd.2014.0824.

[49] M. Zarghami, M. L. Crow, J. Sarangapani, Y. Liu, and S. Atcitty, "A novel approach to interarea oscillation damping by unified power flow controllers utilizing ultracapacitors," *IEEE Trans. Power Syst.*, vol. 25, no. 1, pp. 404–412, 2010, doi: 10.1109/TPWRS.2009.2036703.

[50] H. Soliman and M. Shafiq, "Robust stabilisation of power systems with random abrupt changes," vol. 9, pp. 2159–2166, 2015, doi: 10.1049/iet-gtd.2014.1111.

[51] T. Duong, Y. Jiangang, and V. Truong, "Application of min cut algorithm for optimal location of FACTS

devices considering system loadability and cost of installation," *Int. J. Electr. Power Energy Syst.*, vol. 63, pp. 979–987, 2014, doi: 10.1016/j.ijepes.2014.06.072.

[52] F. C. Jusan, S. Gomes, and G. N. Taranto, "SSR results obtained with a dynamic phasor model of SVC using modal analysis," *Int. J. Electr. Power Energy Syst.*, vol. 32, no. 6, pp. 571–582, 2010, doi: 10.1016/j.ijepes.2009.11.013.

[53] D. Whitley, "A genetic algorithm tutorial," *Stat. Comput. 1994 42*, vol. 4, no. 2, pp. 65–85, Jun. 1994, doi: 10.1007/BF00175354.

[54] J. Kennedy and R. Eberhart, "Particle swarm optimization," *Proc. ICNN'95 - Int. Conf. Neural Networks*, vol. 4, pp. 1942–1948, doi: 10.1109/ICNN.1995.488968.

[55] S. Mirjalili, S. M. Mirjalili, and A. Lewis, "Grey Wolf Optimizer," *Adv. Eng. Softw.*, vol. 69, pp. 46–61, 2014, doi: 10.1016/j.advengsoft.2013.12.007.

[56] S. Mirjalili and A. Lewis, "The Whale Optimization Algorithm," *Adv. Eng. Softw.*, vol. 95, pp. 51–67, May 2016, doi: 10.1016/J.ADVENGSOFT.2016.01.008.

[57] S. Mirjalili, "Dragonfly algorithm: a new meta-heuristic optimization technique for solving single-objective, discrete, and multi-objective problems," *Neural Comput. Appl.*, vol. 27, no. 4, pp. 1053–1073, 2016.

[58] J. S. Chou and D. N. Truong, "A novel metaheuristic optimizer inspired by behavior of jellyfish in ocean," *Appl. Math. Comput.*, vol. 389, p. 125535, 2021, doi: 10.1016/j.amc.2020.125535.

[59] N. J. Berrill, "The Tunicata with an account of the British species." The Ray Society, 1950.

[60] G. H. Davenport, J., Balazs, "'fiery bodies' - are pyrosomas an important component of the diet of leatherback turtles?," vol. 33–38, 1991.

[61] A. J. Lockett, "No free lunch theorems," *Nat. Comput. Ser.*, vol. 1, no. 1, pp. 287–322, 2020, doi: 10.1007/978-3-662-62007-6_12.

[62] L. A.-C. W.W. Nazaroff, *Environmental Engineering Science*, 1 edition. Wiley, New York, 2000.

[63] A. L. S. Mirjalili, S.M. Mirjalili, "Grey Wolf Optimizer," 2014, [Online]. Available: http://dx.doi.org/10.1016/j.advengsoft.2013.12.007.

[64] R. V. Rao, V. J. Savsani, and D. P. Vakharia, "Teaching-learning-based optimization: A novel method for constrained mechanical design optimization problems," *CAD Comput. Aided Des.*, vol. 43, no. 3, pp. 303–315, 2011, doi: 10.1016/j.cad.2010.12.015.

[65] R. P. Parouha and K. N. Das, "A memory based differential evolution algorithm for unconstrained optimization," *Appl. Soft Comput. J.*, vol. 38, pp. 501–517, 2016, doi: 10.1016/j.asoc.2015.10.022.

[66] "Power System Stabilizer (PSS) Definition | Law Insider," [Online]. Available: https://www.lawinsider.com/dictionary/power-system-stabilizer-pss.

[67] F. P. Demello and C. Concordia, "Concepts of Synchronous Machine Stability as Affected by Excitation Control," *IEEE Trans. Power Appar. Syst.*, vol. PAS-88, no. 4, pp. 316–329, 1969, doi: 10.1109/TPAS.1969.292452.

[68] D. A. S. E.V.Larsen, "Applying Power System Stabilizers," *IEEE Trans. Power App. Syst*, vol. PAS-100, pp. 3017–3046, 1981.

[69] J. H. Chow, G. E. Boukarim, and A. Murdoch, "Power System Stabilizers as Undergraduate Control Design Projects," *IEEE Trans. Power Syst.*, vol. 19, no. 1, pp. 144–151, 2004, doi: 10.1109/TPWRS.2003.821003.

[70] Y.Yu, "Electric Power System Dynamics, by," *New York, Acad. Press*, pp. 190–191, 1983.

[71] Starlight Power, "No Title." https://www.dieselgeneratortech.com/generators/what-is-synchronous-

generator.html.

[72] M. A. Pai and A. Stankovic, *Robust Control in Power Systems Series Editors*. .

[73] C. Ussawapusitgul and S. Kaitwanidvilai, “Automatic design of robust PSS for multimachine power system using PSO,” *IEEE Reg. 10 Annu. Int. Conf. Proceedings/TENCON*, pp. 1065–1069, 2011, doi: 10.1109/TENCON.2011.6129274.

[74] P. W. M. P. Sauer, “‘Power system dynamics and stability,’ Urbana, vol. 51,” pp. 34–361, 1997.